PLOS Biology

RESEARCH ARTICLE

# Uracil-driven ROS signaling and larval TrpA1-B neuron activation are required for priming the adult *Drosophila* gustatory response to bacteria

**Romane Milleville**[1], **Gérard Manière**[2*], **Martine Berthelot-Grosjean**[2], **Olivier Lamotte**[2], **Yaël Grosjean**[2], **Julien Royet**[1*], **Cyril Léopold Kurz**[1*]

**1** Aix-Marseille Université, CNRS, IBDM, Marseille, France, **2** Université Bourgogne Europe, Institut Agro, CNRS, INRAE, UMR CSGA, Dijon, France

* gerard.maniere@ube.fr (GM), julien.royet@univ-amu.fr (JR), leopold.kurz@univ-amu.fr (CLK)

Check for updates

OPEN ACCESS

**Citation:** Milleville R, Manière G, Berthelot-Grosjean M, Lamotte O, Grosjean Y, Royet J, et al. (2026) Uracil-driven ROS signaling and larval TrpA1-B neuron activation are required for priming the adult *Drosophila* gustatory response to bacteria. PLoS Biol 24(10): e3004042. https://doi.org/10.1371/journal.pbio.3004042

**Academic Editor:** Piali Sengupta, Brandeis University, UNITED STATES OF AMERICA

**Received:** July 2, 2026

**Accepted:** September 22, 2026

**Published:** October 5, 2026

**Peer Review History:** PLOS recognizes the benefits of transparency in the peer review process; therefore, we enable the publication of all of the content of peer review and author responses alongside final, published articles. The editorial history of this article is available here: https://doi.org/10.1371/journal.pbio.3004042

**Copyright:** © 2026 Milleville et al. This is an open access article distributed under the terms of the Creative Commons Attribution License,

## Abstract

Animals perceive their immediate environment through their sensory systems. While these systems rely on well-defined neuronal circuits and receptor proteins encoded by the genome, they can also be modulated by internal physiological conditions or exogenous factors. We have previously shown that the presence of certain pathogenic bacteria in the larval gut can alter the specificity of bacterial peptidoglycan recognition in the adults that emerge from these larvae. However, the nature of the bacterial signal and the host cells and molecules involved in receiving and transducing this signal remained unknown. Our results identify uracil as the bacterial metabolite responsible for this priming and demonstrate that the effect is mediated by Duox-dependent production of reactive oxygen species (ROS) in the larval gut. We further show that specific expression of TrpA1 isoforms in a Gr66a-expressing neuron of the larval terminal organ is required for the adult response. Together, these findings reveal uracil as the bacterial cue and the Duo/ROS signaling and TrpA1/Gr66a modules as key mediators linking larval gut microbial signals and host integration to subsequent sensory system modulation in the adult.

## Introduction

In natural environments, animals inhabit diverse ecological niches that are colonized by bacteria, viruses, and fungi [1]. Throughout their development and into adulthood, animals interact with, and sometimes host, these microbial co-inhabitants. This close association can be beneficial, as certain microbial communities positively influence vital physiological functions such as fertility, life span, and growth [2–4]. However, some microbes can also negatively impact an animal's health and internal balance [5]. The ability to detect and respond to such potential microbial threats is a fundamental and conserved innate mechanism essential for animal survival. To protect themselves and their offspring, animals have developed refined cellular and humoral

which permits unrestricted use, distribution, and reproduction in any medium, provided the original author and source are credited.

**Data availability statement:** Data Availability: All relevant data are available within the manuscript an its Supporting information files. The data underlying all figures are provided in S1 Data.

**Funding:** Funding: This work was supported by CNRS (https://www.cnrs.fr/fr), ANR (https://anr.fr/) Pepneuron (ANR-21-CE16-0027) to J.R. and Y.G. Research in Y.G.'s laboratory is supported by the CNRS, the "Université de Bourgogne Europe" (https://ube.fr/), the Conseil Régional Bourgogne Franche-Comté (https://www.bourgognefranchecomte.fr/) (PARI grant), the FEDER (European Funding for Regional Economical Development) https://www.europe-en-france.gouv.fr/fr/fonds-europeens-2014-2020/fonds-europeen-developpement-regional-feder), and the European Council (ERC starting grant, GliSFCo-311403) (https://erc.europa.eu/homepage). The funders had no role in study design, data collection and analysis, decision to publish, or preparation of the manuscript. R.M. was paid by through the ANR Pepneuron grant.

**Competing interests:** The authors have declared that no competing interests exist.

**Abbreviations:** CI, confidence Interval; EEC, entero-endocrinal cells; KI, knock-in; PER, Proboscis Extension Reflex; PI, preference index; RLU, relative luminescence units; ROS, Reactive oxygen species; TO, Terminal Organ.

innate immune responses [6]. Defensive responses launched after microbial detection can incur energetic or physiological costs [7,8] and are not always completely effective [9–11]. Early detection of environmental dangers and preparation to confront these threats can complement the canonical immune responses against pathogens and serve as a critical initial defence. The nervous system's ability to perceive microbial threats enables animals to adopt behaviors that mitigate the effects of infection on themselves and their progeny, at either the individual or collective level. Insects such as ants and bees, for example, employ social and behavioral immunity, like grooming, to protect against infection [12–18]. A variety of sensory systems—including smell [19,20] and sight [21,22]—are engaged in detecting biological threats in both vertebrates and invertebrates.

Research on *Drosophila*, has demonstrated that hygienic grooming behaviors can be triggered by fungal molecules or bacterial contact cues, through distinct sensory receptors and neural pathways [23–25]. Volatile compounds, such as geosmin produced by potentially pathogenic fungi, can be detected by insect olfactory receptors and act as repellents that affect food intake and egg laying [20]. Bacteria are characterized by cell wall structures such as peptidoglycan (PGN) or lipopolysaccharide, which serve as crucial ligands for receptors allowing eukaryotes to distinguish them from other organisms [26–29]. Notably, these receptors are found on both immune cells and neurons [30–32].

Multiple studies have shown that bacterial PGN, a core cell wall component, mediates numerous interactions between bacteria and flies [24,31,33–38]. Recognition of PGN by members of the PGRP family activates NF-kB pathways in immune-competent cells, leading to the production of immune effectors and regulators. Recent work has revealed that similar ligand/receptor interactions also maintain a molecular dialogue between bacteria and neurons in the fly's central and peripheral nervous systems [31,34,37]. Hence, PGN detection by adult taste neurons triggers immediate aversive behavior in adult flies. Our recent findings identify two types of gustatory neurons—*ppk23+* and *Gr66a+*—as being essential for this response, though they serve distinct roles. Using time-specific neuronal inactivation and in vivo calcium imaging, we demonstrate that *ppk23+* neurons directly detect PGN in adult flies, whereas *Gr66a+* neurons must be active and possess the transient receptor potential TrpA1 channel during the larval stage to establish PGN sensitivity in adults. Moreover, adult flies that develop from larvae raised in germ-free (axenic) conditions lose the ability to respond to bacterial PGN [37]. Interestingly, reintroducing a single bacterial species, the pathobiont *Levilactobacillus brevis*, but not *Lactiplantibacillus plantarum*, into germ-free larvae—but not into adults—restores this response [37]. Therefore, the larval experience with bacteria influences adult sensory capabilities toward a microbial component. These findings which suggest a larval host-microorganism interaction and integration as well as a critical influence of both genetic and environmental factors during larval development in shaping the sensory capabilities of adult flies, raise two important questions. The first is how the bacterial information acquired by the larva is transmitted through metamorphosis to the future adult. The second, which is the subject of this study, concerns the nature of

the signal provided by only some bacterial species and the mechanisms by which this or these signal (s) prime the larva to give rise to adults capable of sensing PGN through their gustatory neurons, a property absent in germ-free animals.

## Results

### Mutant bacteria that do not release uracil are no longer able to prime larvae

We previously reported that wild-type flies from larvae reared in the presence of *Levilactobacillus brevis (L. brevis) are* attracted to a 1 mM sucrose solution [37]. However, this reflex is considerably attenuated when the sucrose solution contains bacterial peptidoglycan at a concentration of 200 μg/ml, suggesting that PGN has a bitter valence for adult flies (Figs 1A, S1A, and S1B and [37]). We have previously demonstrated that PGN derived from bacteria is perceived by *ppk23+* neurons located in the proboscis of adult flies and triggers aversion. We also showed that adults derived from larvae raised under axenic conditions lose this capacity while continuing to react to caffeine, an aversive molecule, demonstrating that their gustatory system remains functional. Furthermore, the induced cohabitation of axenic larvae with *L. brevis*, but not with *Lactiplantibacillus plantarum*, is sufficient to restore the aversive response to PGN in adults [37]. This suggests that certain specific bacterial species can prime larvae to give rise to PGN-sensitive adults (S1A Fig). To identify the nature of the bacterial priming signal(s), we used a mono-association protocol in which axenic larvae are reared in the presence of the desired bacterial strains or compounds. Emerged adults are tested for their ability to respond to PGN using the proboscis extension reflex (PER) as a read out for the gustatory response (S1B Fig). While larval cultivation with *L. brevis* primes the animals, neither heat-killed *L. brevis* nor the supernatant of a *L. brevis.* solution were able to reproduce the priming effects of live *L. brevis* (Fig 1A). In order to search for a putative priming inducer, we looked for molecular characteristics present in bacterial species capable of priming but absent in others. While, as mentioned above, the opportunistic pathobionts *L. brevis* is capable of priming axenic larvae, *L. plantarum*, considered a symbiont for *Drosophila*, is not [37]. As previous reports demonstrate that the nucleoside catabolism pathway controlling bacterial uracil is an essential trigger for the transition from commensal to pathogen [39,40], we tested whether it could also be involved in the priming of axenic larvae. To this end, and for the remainder of the study, we used *Erwinia carotorova* (also known as *Pectobacterium carotovorum*, strain *Ecc*$^{15}$) for which valuable mutants with impact on uracil metabolism had previously been generated [41,42]. Unlike wild-type bacterial strains that were capable of larval priming, two mutants (*Ecc*$^{15}$Δ4 and *Ecc*$^{15}$*pyrE::Tn5*) whose ability to release uracil is impaired, lost this property (Fig 1B). This result, which suggests that uracil is involved in priming, was confirmed by experiments showing that simply adding purified uracil at 1mM to the medium is sufficient to trigger priming in larvae raised under axenic conditions (Fig 1B).

Loss of priming in uracil-release mutants and sufficiency of exogenous uracil implicate uracil as a key determinant under our conditions. To delineate whether uracil-related molecules could prime larvae, we used the same protocol as the one involving uracil to expose sterilized eggs to cytosine or thymine. None of these molecules were able to phenocopy the priming effect of uracil (Figs 1B and S2).

In the monoassociation protocol, bacteria or chemical compounds are deposited onto sterilized eggs, and the resulting adults are subsequently tested for PER. In our previous study investigating the PER response to a sucrose + PGN mixture and the requirement for larval exposure to bacteria, we identified a critical developmental window between oviposition and 48 h post-oviposition [37]. We therefore asked whether the effect of uracil depended on the same critical period. To address this question, we exposed 24h-old larvae derived from sterilized eggs to uracil rather than exposing the eggs themselves, and subsequently assayed PER in the resulting adults. This treatment failed to prime the larvae (Fig 1B). We obtained the same results with 24 h-old larvae derived from sterilized eggs and exposed to *Ecc*$^{15}$. These results confirm the existence of a critical developmental window and further narrow it to a period occurring before 24 h after larval hatching.

Our previous report, together with the present study, establishes a link between larval experience and the ability of adult flies to discriminate between a food mixture containing sucrose alone and one containing sucrose supplemented

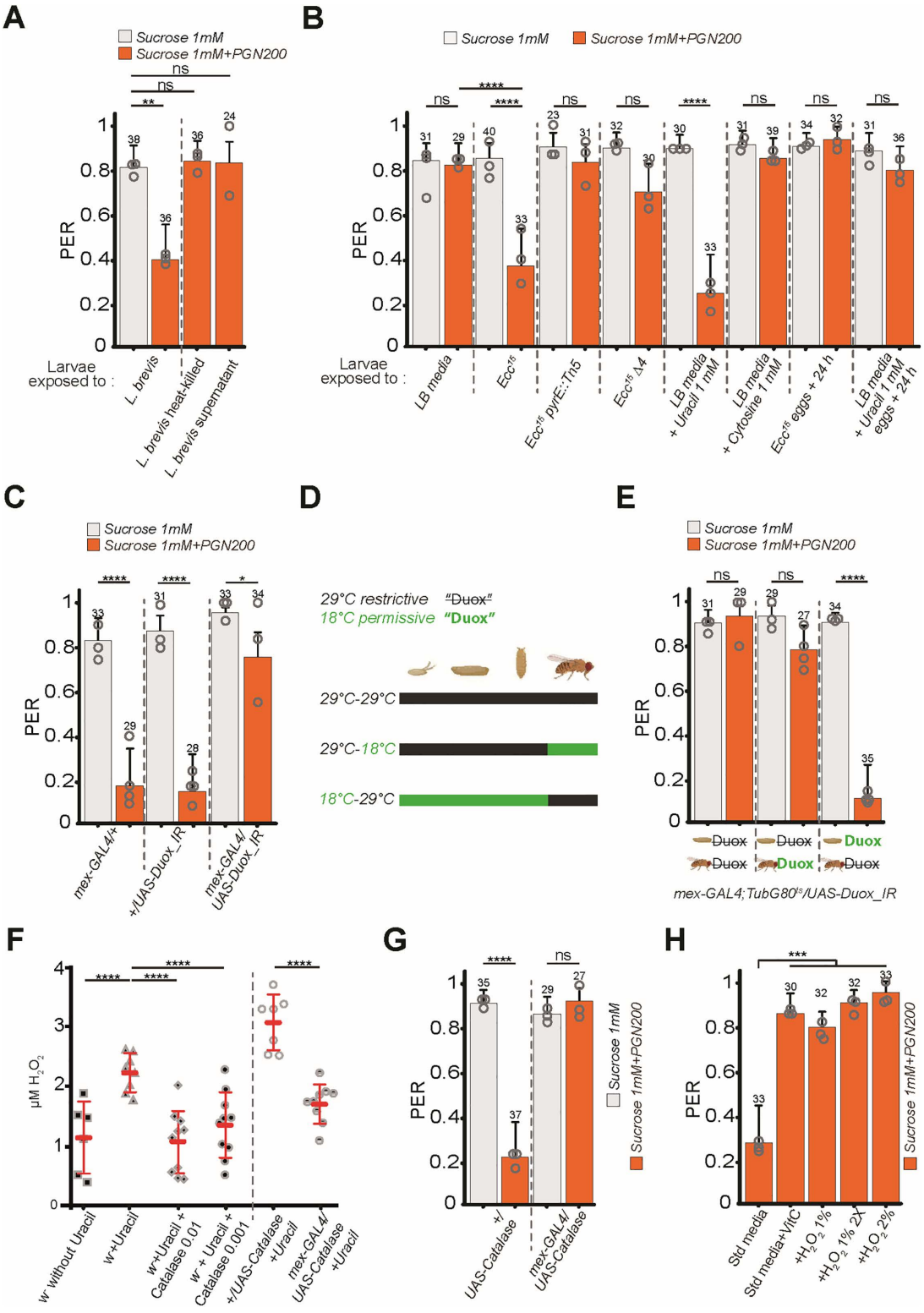



**Fig 1. Larval exposure to uracil is required for adult PGN-mediated inhibition of PER. (A)** Live *L. brevis* are necessary and sufficient to prime the larvae. Sterilized eggs were exposed to live or dead bacteria as well as supernatant. The resulting adults were raised on antibiotics-containing

media (ATB). PER index of $w^-$ flies to control solutions of sucrose (Sucrose 1 mM) and sucrose + PGN from *E. coli* K12 (Sucrose 1mM + PGN200) were obtained. **(B)** Uracil is necessary and sufficient to prime the larvae. Sterilized eggs were exposed to the different treatments and the resulting adults raised on antibiotics-containing media (ATB). Specifically, eggs were either monoassociated with bacterial strains, or exposed to LB media or to LB media containing uracil or cytosine. Addition of uracil or $Ecc^{15}$ 24h after sterilized egg deposition was tested. The resulting adults were raised on antibiotics-containing media (ATB). PER index of $w^-$ flies to control solutions of sucrose and sucrose + PGN from *E. coli* K12 at 200 μg/mL (PGN200) were obtained. **(C)** The Duox enzyme is necessary in enterocytes for the priming. PER index to solutions of sucrose and sucrose + PGN (PGN200) of *GAL4* (*mex-GAL4*/+) and *UAS (+/UAS-Duox_IR*) control flies as well as animals with the *Duox* transcript impaired via RNAi in enterocytes (*mex-GAL4/UAS-Duox_IR*) were calculated. Larvae were raised on conventional media and the resulting adults raised on antibiotics-containing media. **(D)** Graphical representation of the life periods during which flies are shifted from 18 °C to 29 °C for a stage-dependent RNAi assay. The ubiquitously expressed *Tub-G80$^{ts}$*, that inhibits the activity of GAL4, is temperature-sensitive: the GAL4 inhibitor is active at 18 °C (green) and inactivated at 29 °C (black), its inactivation allows the expression of any *UAS*. In the case of *mex-GAL4*; *TubG80$^{ts}$/UAS-Duox_IR*, at 18 °C the *Duox* transcripts will not be impaired (Duox) while it will be at 29 °C. **(E)** Duox activity in enterocytes is necessary during the larval life for priming. PER index to solutions of sucrose and sucrose + PGN (PGN200) of *mex-GAL4; TubG80$^{ts}$/UAS-Duox_IR* flies with the *Duox* transcript impaired all-life long, only during the larval stages or only during the adult stage were calculated. Larvae were raised on conventional media and the resulting adults raised on antibiotics-containing media. **(F)** $H_2O_2$ is detectable within the larvae 24 h following exposure to uracil 1 mM. Sterilized eggs were exposed to LB media or to LB media containing uracil. Twenty-four h later, the concentration of $H_2O_2$ within the animals was quantified. To confirm that $H_2O_2$ is the quantified product, catalase (0.01 U/mL and 0.001 U/mL) was applied to the samples from uracil-exposed larvae or overexpressed in enterocytes (*mex-GAL4/UAS-Catalase*). **(G)** Reducing the amount of ROS impairs the priming. PER index to solutions of sucrose and sucrose + PGN (PGN200) of *UAS (+/UAS-Catalase*) control flies as well as animals with the Catalase over-expressed in enterocytes (*mex-GAL4/UAS-Catalase*) were obtained. Larvae were raised on conventional media and the resulting adults raised on antibiotics-containing media. **(H)** $H_2O_2$ supplementation to larvae is not sufficient to prime while vitamin C (VitC) addition during the larval life prevents it. PER index to solutions of sucrose + PGN (PGN200) of $w^-$ flies was calculated. Larvae were raised on conventional media with or without vitamin C (0.2 mg/mL) or on monoassociation media with or without $H_2O_2$ (1% on eggs or 1% on eggs then 1% on 24h-larvae (2X) or 2% on eggs). All the resulting adults were raised on antibiotics-containing media. PER index of $w^-$ flies to solutions of sucrose + PGN from *E. coli* K12 at 200 μg/mL (PGN200) was obtained. The PER index is calculated as the percentage of flies tested that responded with a PER to the stimulation ± 95% confidence interval (CI). A PER value of 1 means that 100% of the tested flies extended their proboscis following contact with the mixture, a value of 0.2 means that 20% of the animals extended their proboscis. The number of tested flies (*n*) is indicated on top of each bar. For each condition, at least 3 groups with a minimum of 10 flies per group were used. Each independent group is represented as an open circle. ns indicates $p > 0.05$, * indicates $p < 0.05$, ** indicates $p < 0.01$, *** indicates $p < 0.001$, **** indicates $p < 0.0001$ Fisher's exact test. Further details can be found in the detailed lines, conditions and, statistics for the figure section. The data underlying this Figure can be found in S1 Data. Created in BioRender. Kurz, L. (2026). https://core.local.biorender.dev/api/short-link/9ojribp.

https://doi.org/10.1371/journal.pbio.3004042.g001

with PGN. We demonstrated that this discrimination relies on a subset of *ppk23+* neurons located in the adult proboscis. Exposure to PGN induced a measurable increase in intracellular calcium levels in these neurons, indicating their activation by bacterial cues. In contrast, *ppk23+* neurons from adults derived from larvae not exposed to bacteria failed to respond to PGN stimulation [37].

To investigate whether larval priming with uracil could modulate the responsiveness of adult *ppk23+* neurons, we performed GCaMP calcium imaging experiments. Specifically, we compared the neuronal responses to PGN in adults originating from larvae exposed to uracil with those in adults derived from non-exposed larvae. This approach allowed us to examine, at the cellular level, how early-life exposure to microbial-associated signals influences the development of sensory discrimination mechanisms in adulthood. While *ppk23+* proboscis's neurons of adults from larvae exposed or not to uracil responded to salt (positive controls), only the adults originating from uracil-exposed larvae responded to PGN (S3 Fig), supporting the idea that larval experience influences neuronal responsiveness later in adulthood.

### The production of reactive oxygen species by enterocytes is necessary for larval priming

Previous studies demonstrate that uracil acts as a microbe-derived factor that modulates intestinal immunity in *Drosophila* [39]. Uracil-dependent activation of Duox leads to the production in the intestinal tract of reactive oxygen species (ROS), which combat invading pathobionts but also induce damage to host tissues [42–44]. It has been shown that the inactivation of a single bacterial gene involved in uracil production is sufficient to induce a phenotypic change from a colitogenic bacterium to a commensal bacterium [41]. These results, which demonstrate the importance of Duox-dependent ROS production in mediating the effects of uracil, prompted us to test whether ROS were also involved in larval priming. To do this, we induced RNA interference-mediated reduction of *Duox* transcripts specifically in enterocytes using the *mex-GAL4*

driver (S4 Fig). While control adult strains showed the described aversion to PGN in the PER test, this was no longer the case for *mex-GAL4*/*UAS-Duox_IR* adult flies (Fig 1C). Taking advantage of the *GAL4*/*GAL80$^{ts}$* binary system, we reduced ROS levels in either the larval or adult stage (Fig 1D and 1E). While reducing ROS levels in larval guts suppressed priming, this was not the case when the reduction was induced in the adult stage (Fig 1E). Based on the genetic data and the identified critical period, we tested whether ROS, and $H_2O_2$ in particular, could be detected in 24-h-old larvae following exposure of sterilized eggs to uracil. To confirm that the measured signal corresponded to $H_2O_2$, we either treated uracil-exposed samples with catalase or genetically overexpressed catalase (an enzyme that degrades hydrogen peroxide) in enterocytes (*mex-GAL4*/*UAS-Catalase*). Our results demonstrate that $H_2O_2$ levels are increased following uracil exposure (Fig 1F). Interestingly, priming in larvae was suppressed by *GAL4*/*UAS*-mediated overexpression of catalase, in the gut (Fig 1G). Similarly, the addition of the antioxidant vitamin C (VitC) to the medium at a non-bactericidal concentration (S5A Fig) suppressed larval priming (Fig 1H). However, using either the monoassociation protocol (S1B Fig) or axenic media (ATB), neither a single application of 1% $H_2O_2$ (on eggs only) nor two applications (on eggs and 24-h-old larvae; 2×), nor 2% $H_2O_2$, were sufficient to induce priming (Figs 1H, S5B, and S5C). Overall, these results support a model in which uracil triggers in larvae a Duox-dependent ROS production in larval enterocytes required for priming.

### The B, C, and E isoforms of TrpA1, but not the A and D, are involved in larval priming

Our previous data demonstrate that expression of the TrpA1 ion channel in larval *Gr66a+* neurons is necessary for larval priming by bacteria [37]. *Drosophila* TrpA1, which shares conserved sensory functions with its mammalian ortholog and is activated by heat, ROS, UV light, and irritant chemicals (Fig 2A), is alternatively spliced to produce five isoforms (Fig 2B) [45–50]. By generating and phenotypically analyzing knock-in (*KI*) flies expressing a single TrpA1 isoform and knock-out flies (*KO*) lacking selected TrpA1 isoforms, Gu and colleagues conclude that a given sensory stimulus preferentially activates a specific TrpA1 isoform in vivo [45]. Using this genetic toolkit, we sought to identify the number and nature of TrpA1 isoform (s) involved in larval priming to bacteria. Although these *TrpA1* mutants all responded similarly to sucrose, their PER to a sucrose + PGN solution differs. Among the *KI* lines, *B-KI*, *C-KI*, and *E-KI* flies reacted like the wild type. In contrast, flies expressing only isoform *A* or *D* showed a response similar to that of *TrpA1-KO* mutant flies, demonstrating that they lack the ability to mediate larval priming. These results, which suggest that isoforms *B*, *C*, and *E*, but not *A* and *D*, are capable of priming, were confirmed by analysis of the different *KO* mutant flies (Fig 2C). Adults from lines in which at least one of the three competent isoforms was present (*E-KO*, *BC-KO*, and *AD-KO*) all responded to PGN like the controls. This result was consistent with the fact that *BCE-KO* flies, which lack all three competent isoforms (*B*, *C* and *E*), were the only flies whose ability to respond to PGN was impaired (Fig 2C). These results demonstrate that expression of any one of the three isoforms, *B, C*, or *E* is sufficient to ensure larval priming. The simplest explanation would be that B, C, and E are functionally redundant and share a functional property that is absent in isoforms A and D. Careful examination of the TrpA1 peptides suggests that this is not the case. Indeed, no protein domain that is specifically present in proteins TrpA1 B, C, and E but absent in A and D could be identified. An alternative hypothesis would be that the type of cells(s) in which the *TrpA1* isoforms are expressed is the important criterion to consider and that isoforms *B*, *C* and *E* are co-expressed in one or more cells that would be necessary to ensure TrpA1-dependent priming. It should be noted that these two hypotheses (the nature of the peptides or the domain of expression) are not mutually exclusive (see below).

### *TrpA1 B, C* and *E* isoforms are co expressed in some anterior neurons

As expected from a functionally pleiotropic protein, *TrpA1* is expressed in many cell types in both larvae and adults. In addition, Gu and colleagues, have previously shown that each *TrpA1* isoform has a unique expression pattern and that multiple isoforms are often co-expressed in the same cells. To investigate whether the shared ability to prime of B, C, and E isoforms can be attributed to their co-expression in some functionally important cells, we looked for cells that would express all 3 isoforms. For that, we crossed the *TrpA1*-isoform-*GAL4* flies with *UAS-gfp* and compared their expression

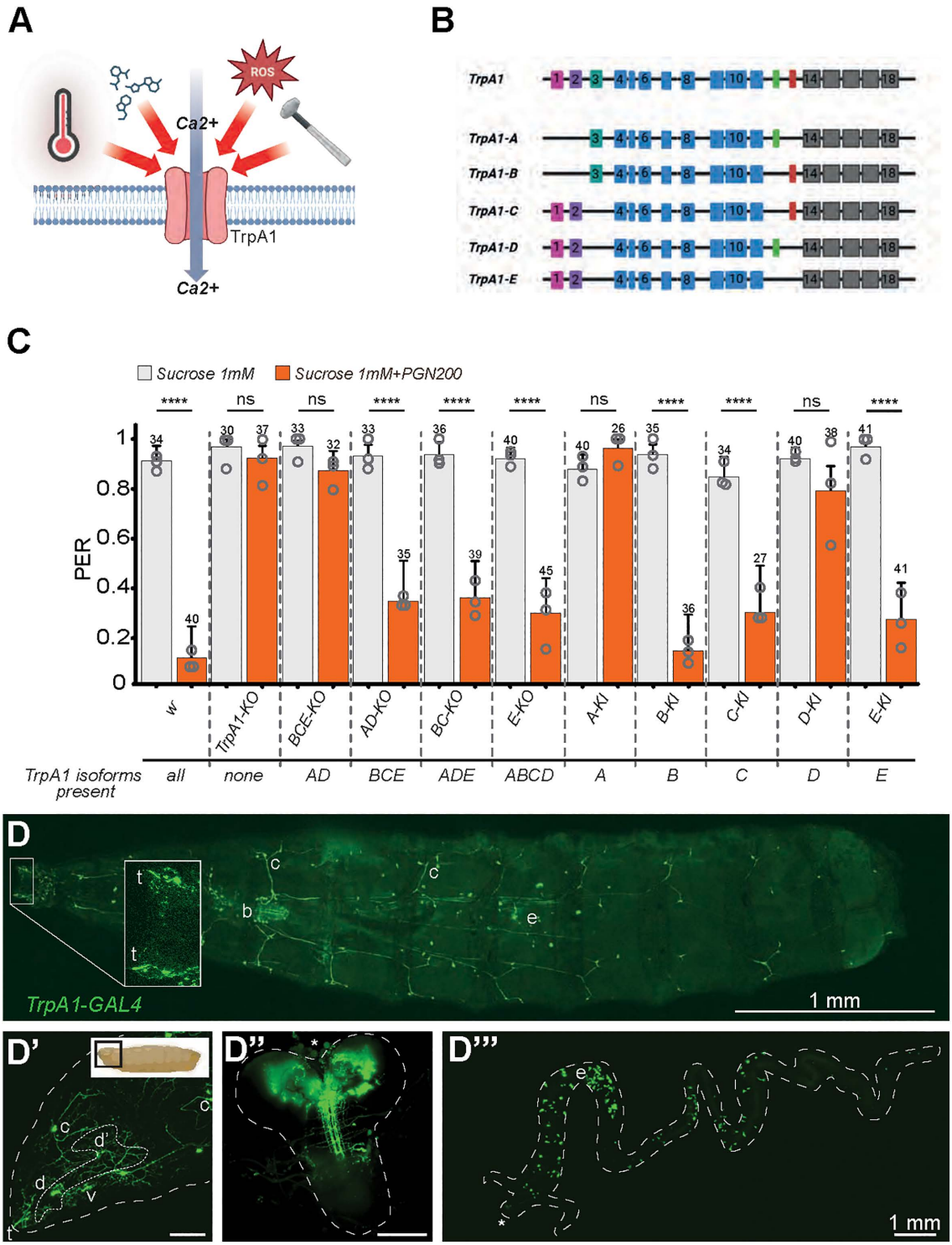



**Fig 2. TrpA1 and specifically the B, C and E isoforms are involved in the priming. (A)** Graphical representation of the TrpA1 channel responding to various stimuli through the entry of ions into the cell. Heat, specific chemicals, ROS and mechanical stimuli trigger the TrpA1 proteins participating to the generation of an action potential. **(B)** Graphical representation of the *TrpA1* gene (top) with colored boxes representing exons and colors related to functional domains of the translated protein. Five spliced variant isoforms have been reported so far, they all share exons 4–11 and exons 13–18. **(C)** *TrpA1-B*, *-C* and *-E* isoforms are involved in priming. PER index to solutions of sucrose and sucrose + PGN (PGN200) of control flies as well as *KO*

and *KI* animals for the *TrpA1* isoforms was calculated. Depending on the genotype of the tested animal, the *TrpA1* isoforms that are present are listed under the x-axis. (**D–D‴**) The *TrpA1-GAL4* driver (pan-isoforms) is widely expressed. Confocal images of larvae expressing *gfp* under the control of the pan-isoforms *TrpA1-GAL4* driver with a whole L3 larvae **(D)**, the anterior part of a larvae with anteriormost on the left (**D′**), the larval brain (**D″**) and the gut (**D‴**). In **(D)**, the larger rectangle is a magnification of the most anterior part of the animal housing two *gfp*+ symmetrical neurons whose dendrites extend toward the external environment (t). (b) is for brain, (c) is for C4da neurons, (d) is for dorsal pharyngeal sensilla ganglion, (d′) is for dorsal pharyngeal organ ganglion, (v) is for ventral pharyngeal sensilla ganglion and (e) is for entero-endocrinal cells. In **D′** and **D″**, the scale bar represents 100 μm. In **D′** and **D″**, the asterisk indicates the anterior part of the organ. A schematic representation of the whole larva indicates the depicted area. The PER index is calculated as the percentage of flies tested that responded with a PER to the stimulation ± 95% confidence interval (CI). A PER value of 1 means that 100% of the tested flies extended their proboscis following contact with the mixture, a value of 0.2 means that 20% of the animals extended their proboscis. The number of tested flies (*n*) is indicated on top of each bar. For each condition, at least 3 groups with a minimum of 10 flies per group were used. Each independent group is represented as an open circle. ns indicates $p > 0.05$, * indicates $p < 0.05$, ** indicates $p < 0.01$, *** indicates $p < 0.001$, **** indicates $p < 0.0001$ Fisher's exact test. Further details can be found in the detailed lines, conditions and, statistics for the figure section. The data underlying this Figure can be found in S1 Data. Created in BioRender. Kurz, L. (2026). https://core.local.biorender.dev/api/short-link/9ojribp.

https://doi.org/10.1371/journal.pbio.3004042.g002

domain. Interestingly, all 3 isoforms were expressed in a single and isolated anteriormost neuron probably belonging to one of the bitter neurons of the sensory terminal organ (TO) and in few neurons of the Dorsal and Ventral organs (Figs 2D and 3A–3C–3C). Additionally, all three isoforms were also expressed in the horseshoe-shaped BLP larval brain neurons that have been shown to play a role in thermal nociception [51], while only *C* and *E* were expressed in the larval VNC (Figs 3D–3F). Finally, all three isoforms and the pan-isoforms were expressed in gut cells, which are likely to be entero-endocrinal cells (EEC) (Figs 2D and 3G–3I–3I). However, while as reported earlier, *TrpA1-C* and *TrpA1-E* were expressed in C4da larval nociceptors neurons [45], it was not the case for *TrpA1-B* (S6 Fig).

Since the *TrpA1-B KI* line has the most restricted expression pattern of the 3 reporter lines with no expression in the VNC and in the C4da larval nociceptors neurons, we further focused on this line. We first confirmed, via RNAi-mediated downregulation, that *TrpA1* inactivation in the larval but not the adult *TrpA1-B-GAL4* expression domain was sufficient to block priming (Fig 4A and 4B). This result, together with those previously reported, demonstrate that inactivating *TrpA1* in either *Gr66a-GAL4* [37] or in *TrpA1-B-GAL4* larval cells prevent larval priming. This suggests that *TrpA1-B-GAL4* and *Gr66a-GAL4* are co-expressed in one or more cells in which *TrpA1* expression would be required for priming. *TrpA1* expression in bitter-sensing GRNs, including *Gr66a+* neurons, has been well established in adults [48,52,53].

Consistently, using the binary system *GAL4*/*UAS* and *LexA*/*LexAop*, we showed that one of the three Gr66a-positive neurons is *TrpA1-B-GAL4* (Figs 4C, 4C′ and 4C″). We also excluded the gut part as being essential for priming since *Gr66a-GAL4* is not expressed in the gut ([37] and S7 Fig). To further identify the neuron(s) and the TrpA1 isoform mediating priming, we try to rescue the pan-isoform *TrpA1* mutant by providing different *TrpA1* isoforms in *Gr66a+* neurons. While the ability to prime that is lost in *TrpA1* mutant was fully rescued by expressing *TrpA1-B* in *Gr66a+* cells, this was not the case for *TrpA1-A* (Figs 4D and S8). Altogether, these results have several implications. (i) they demonstrate that the larval neurons and not the enteroendocrine cells are required for priming (ii) they demonstrate that the expression of *TrpA1-B* in *Gr66a+* cells is sufficient for priming (iii) they strongly suggest that the *TrpA1-B+*/*Gr66a+* anterior neuron is the cell in which *TrpA1-B* (or probably either *C* and *E*) need to be expressed to allow priming (iv) they demonstrate that all the *TrpA1* isoforms are not functionally substitutable as far as priming is concerned. All of these results were confirmed using another *GAL4* line (*Gr39a.b*), whose expression pattern in the larvae resembles that of *TrpA1-B* (S9A Fig) and which is not expressed in the EEC (S9C Fig). Co-expression confirmed that one of the *Gr39a.b-GAL4* TO neurons is *TrpA1-B* positive (S9B Fig). Moreover, impairing *TrpA1* expression in the *Gr39a.b-GAL4* cells that do not include EEC was sufficient to abrogate the adult PGN avoidance phenotype observed in controls (Fig 4E).

### The *TrpA1-B* positive TO neuron is activated by $H_2O_2$

After identifying, on the one hand, that *TrpA1-B* expression in the *TrpA1-B+*/*Gr66a+* anterior neuron is necessary for priming and, on the other hand, that ROS are also involved, we hypothesized that the latter could be the signal activating

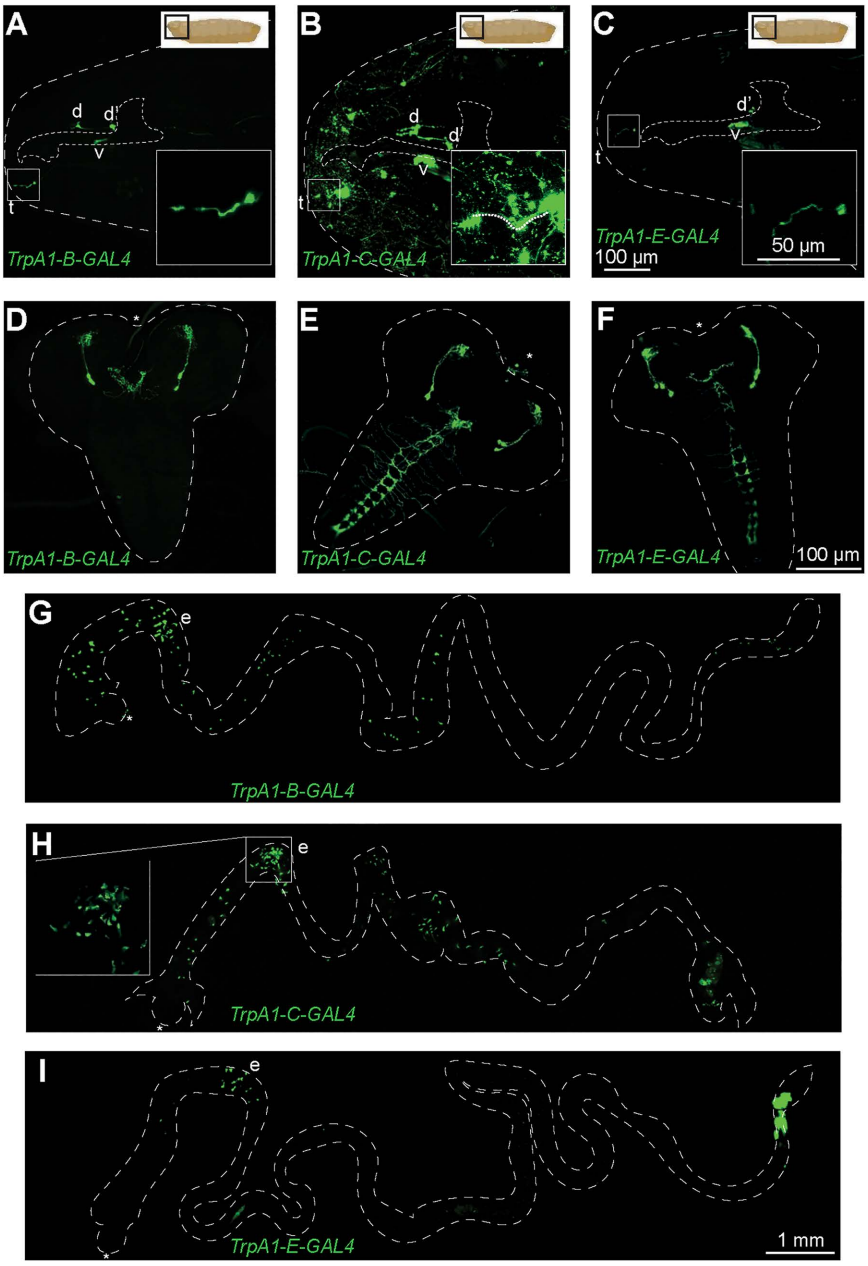



**Fig 3. The expression pattern of the B isoform contains all the elements common to isoforms B, C and E.** (**A–I**) Confocal images of larvae expressing *gfp* under the control of the *TrpA1-B-GAL4* driver (**A**, **D** and **G**), the *TrpA1-C-GAL4* driver (**B**, **E** and **H**) or the *TrpA1-E-GAL4* driver (**C**, **F** and **I**). Shown are the anterior parts **(A–C)**, the brains (**D–F**) and the guts (**G–I**). In **(A–C)**, the anterior is on the left and the larger square is a magnification of the most anterior part of the animal housing a neuron whose dendrite extends toward the external environment (t). In (**D–I**), the asterisk indicates the anterior part of the organ. (b) is for brain, (c) is for C4da neurons, (d) is for dorsal pharyngeal sensilla ganglion, (d′) is for dorsal pharyngeal organ ganglion, (v) is for ventral pharyngeal sensilla ganglion and (e) is for entero-endocrinal cells. In **(B)**, strong *gfp* expression in C4da neurons makes it difficult to distinguish other transgene-expressing cells, but the neuron extending its dendrite toward the external environment is still detectable and outlined in the larger square. A schematic representation of the whole larva indicates the depicted area. Created in BioRender. Kurz, L. (2026). https://core.local.biorender.dev/api/short-link/9ojribp.

https://doi.org/10.1371/journal.pbio.3004042.g003

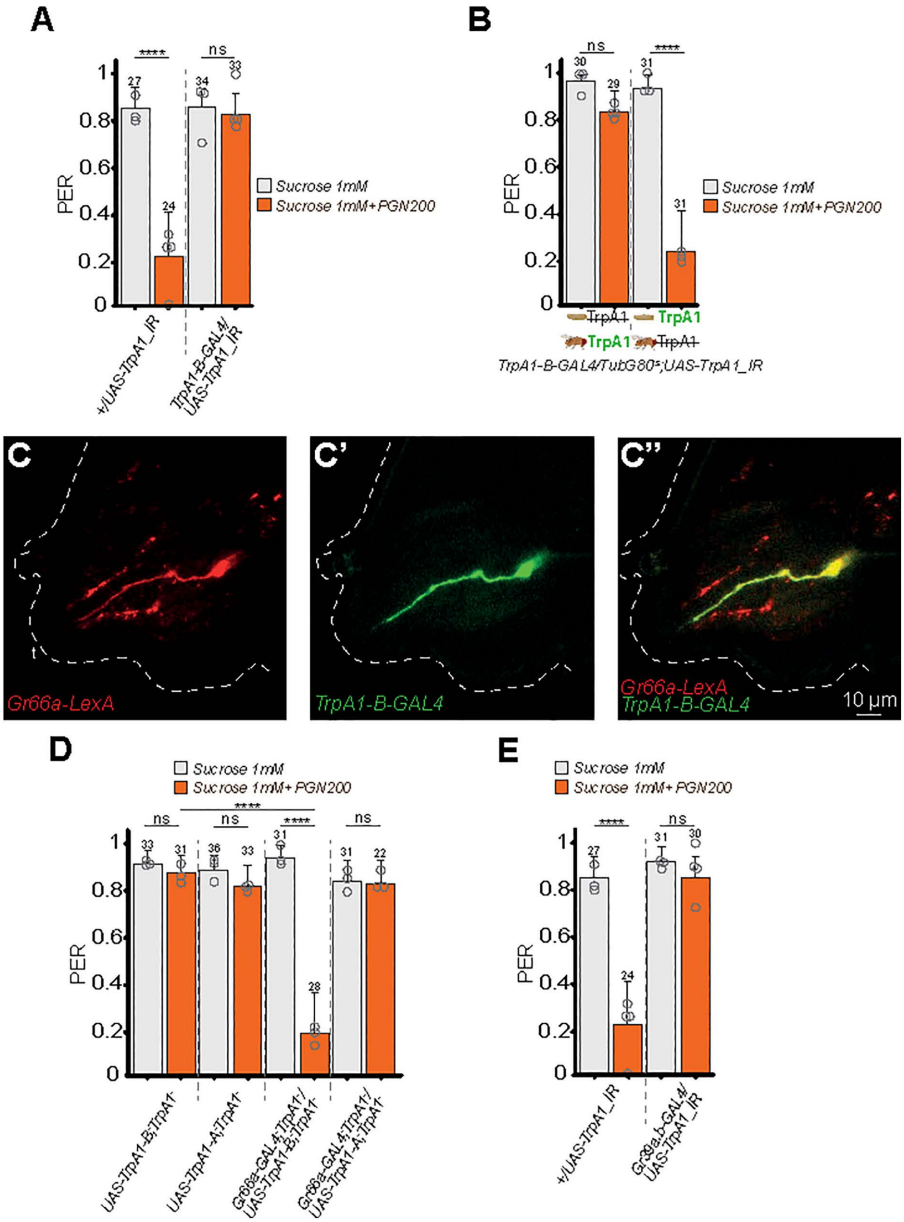



**Fig 4.** ***TrpA1-B+* cells are *Gr66a+* as well as necessary for priming with the TrpA1-B isoform sufficient. (A)** TrpA1 is necessary for priming in *TrpA1-B+* cells. PER index to solutions of sucrose and sucrose + PGN (PGN200) of control flies *(+/UAS-TrpA1_IR*) as well as animals with the *TrpA1* transcripts impaired via RNAi in *TrpA1-B+* cells (*TrpA1-B-GAL4/UAS-TrpA1_IR*) was calculated. Larvae were raised on conventional media and the resulting adults raised on antibiotics-containing media. **(B)** *TrpA1* is necessary for priming in *TrpA1-B+* cells only during larval stage. PER index to solutions of sucrose and sucrose + PGN (PGN200) of *TrpA1-B-GAL4; TubG80$^{ts}$/UAS-TrpA1_IR* animals with the *TrpA1* transcripts impaired via RNAi in *TrpA1-B+* cells only during the larval stages (left) or only during the adult stage (right) was calculated. Larvae were raised on conventional media and the resulting adults raised on antibiotics-containing media. (**C–C″**) Confocal images of the anterior part of a representative larva expressing *mCherry* under the control of the *Gr66a-LexA* driver as well as *gfp* under the control of *TrpA1-B-GAL4* driver. In **C**, dendrites from three *Gr66a+* neurons are detectable, but only one cellular body is clearly visible. **(D)** *TrpA1-B* isoform is sufficient for priming in *Gr66a+* cells while *TrpA1-A* is not. PER index to solutions of sucrose and sucrose + PGN (PGN200) of control flies impaired for priming (*UAS-TrpA1-B; TrpA1$^{-}$* and *UAS-TrpA1-A; TrpA1$^{-}$*) as well as animals with the *TrpA1* transcripts over-expressed only in *Gr66a+* cells in the *TrpA1$^{-}$* mutant background (*Gr66a-GAL4; TrpA1$^{-}$/UAS-TrpA1-B; TrpA1$^{-}$* and *Gr66a-GAL4; TrpA1$^{-}$; UAS-TrpA1-A; TrpA1$^{-}$*) was calculated. Larvae were raised on conventional media and the resulting adults raised on antibiotics-containing media. **(E)** Impairing *TrpA1* expression in *Gr39a.b+* cells prevent priming. PER index to solutions of sucrose and sucrose + PGN (PGN200) of control flies (*+/UAS-TrpA1_IR*). Larvae were raised on conventional media and the resulting adults raised on antibiotics-containing media. The *+/UAS-TrpA1_IR*

data from Fig 4E are those present on Fig 4A. The PER index is calculated as the percentage of flies tested that responded with a PER to the stimulation ± 95% confidence interval (CI). A PER value of 1 means that 100% of the tested flies extended their proboscis following contact with the mixture, a value of 0.2 means that 20% of the animals extended their proboscis. The number of tested flies (*n*) is indicated on top of each bar. For each condition, at least 3 groups with a minimum of 10 flies per group were used. Each independent group is represented as an open circle. ns indicates $p > 0.05$, * indicates $p < 0.05$, ** indicates $p < 0.01$, *** indicates $p < 0.001$, **** indicates $p < 0.0001$ Fisher's exact test. Further details can be found in the detailed lines, conditions and, statistics for the figure section. The data underlying this Figure can be found in S1 Data.

https://doi.org/10.1371/journal.pbio.3004042.g004

the former. To test this model, we used calcium imaging to measure the ability of *Gr66a+* and *TrpA1+* anterior neurons to respond to $H_2O_2$. When larvae expressing *Gr66a-GAL4*/*UAS-GCaMP* were stimulated with a 1% $H_2O_2$ solution, only one of the three anterior neurons responded strongly to the stimuli (Fig 5A–5D). Interestingly, the neuron that responded to $H_2O_2$ was the only one to respond to quinine (Figs 5D and S10A–S10F). Using the same approach, we were able to show that the TO *TrpA1-B-GAL4* neuron was activatable by $H_2O_2$ and that this response was abrogated if *TrpA1* transcripts were cell-specifically downregulated (Fig 5E–5H). Having demonstrated that this larval neuron was required for priming and can be activated by quinine, we tested whether larval exposure to quinine using the monoassociation protocol was sufficient to prime larvae, as previously shown for uracil, and found that it was not (S10G Fig). These results support that a single TO *TrpA1+*/*Gr66a+* neuron contributes to larval priming and is directly activated by ROS in a TrpA1-dependent manner.

### Uracil induces a Duox-dependent signal activating *TrpA1-B+* neurons in naïve larvae

To validate our model that uracil released by bacteria activates intestinal Duox resulting in the production of ROS that are then detected by the anteriormost *TrpA1-B+* neuron, we tested whether larvae exposed to uracil could release a Duox-dependent signal capable of activating *TrpA1-B+* neurons in naïve individuals, i.e., larvae that had not been exposed to uracil or any prior stimulating cue (*TrpA1-B-GAL4*/*UAS-GCaMP*). To do so, larvae reared on antibiotic-containing food were transferred to liquid medium and incubated with 1 mM uracil or water for 3 hours. The resulting conditioned medium was assayed for calcium responses in naïve, non–uracil-exposed animals (Fig 6A). Strikingly, while neither uracil alone nor water from larvae not exposed to uracil induced any response, the medium conditioned by uracil-treated larvae triggered a calcium rise in the anteriormost *TrpA1-B+* neuron (Figs 6B, 6C, and S11). Importantly, when *Duox* expression was specifically reduced in enterocytes of the uracil-treated larvae (*mex-Gal4*/*UAS-Duox_IR*), the conditioned medium no longer activated the *TrpA1-B+* neuron (Fig 6B and 6C).

To determine whether ROS is produced by larvae under these conditions and to characterize its time course, we measured ROS levels over time using a chemiluminescent probe in wells containing exposed larvae. Larvae exposed to buffer exhibited a basal level of ROS that remained stable over the course of the experiment (Fig 6D). This signal was abolished upon addition of vitamin C (VitC). In contrast, addition of uracil triggered an increase in ROS compared to buffer alone; this signal then gradually decreased over time. At 3 hours, ROS levels following uracil exposure remained higher than in the buffer condition. These results indicate that uracil exposure generates a Duox-dependent signal in donor larvae—likely a ROS such as $H_2O_2$—that can activate *TrpA1-B+* neurons in naïve recipients.

### Free-feeding assays confirm PGN avoidance and reveal its dependence on larval microbial exposure and TrpA1

Using the PER method, we showed that adult avoidance of PGN relies on larval exposure to bacteria that produce uracil and is mediated by ROS and specific TrpA1 isoforms in host *Gr66a+* neurons. However, since proboscis extension reflects only one stage of a complex feeding sequence involving smell, tarsal detection, ingestion, and pharyngeal evaluation, we asked whether this aversion also manifests in a more physiological and ecologically relevant context. We therefore turned to a two-choice free-feeding paradigm in which flies can move freely, explore the environment, and voluntarily ingest the substrate of their choice. Using a 96-well assay with colored agar [54], we assessed preference by scoring

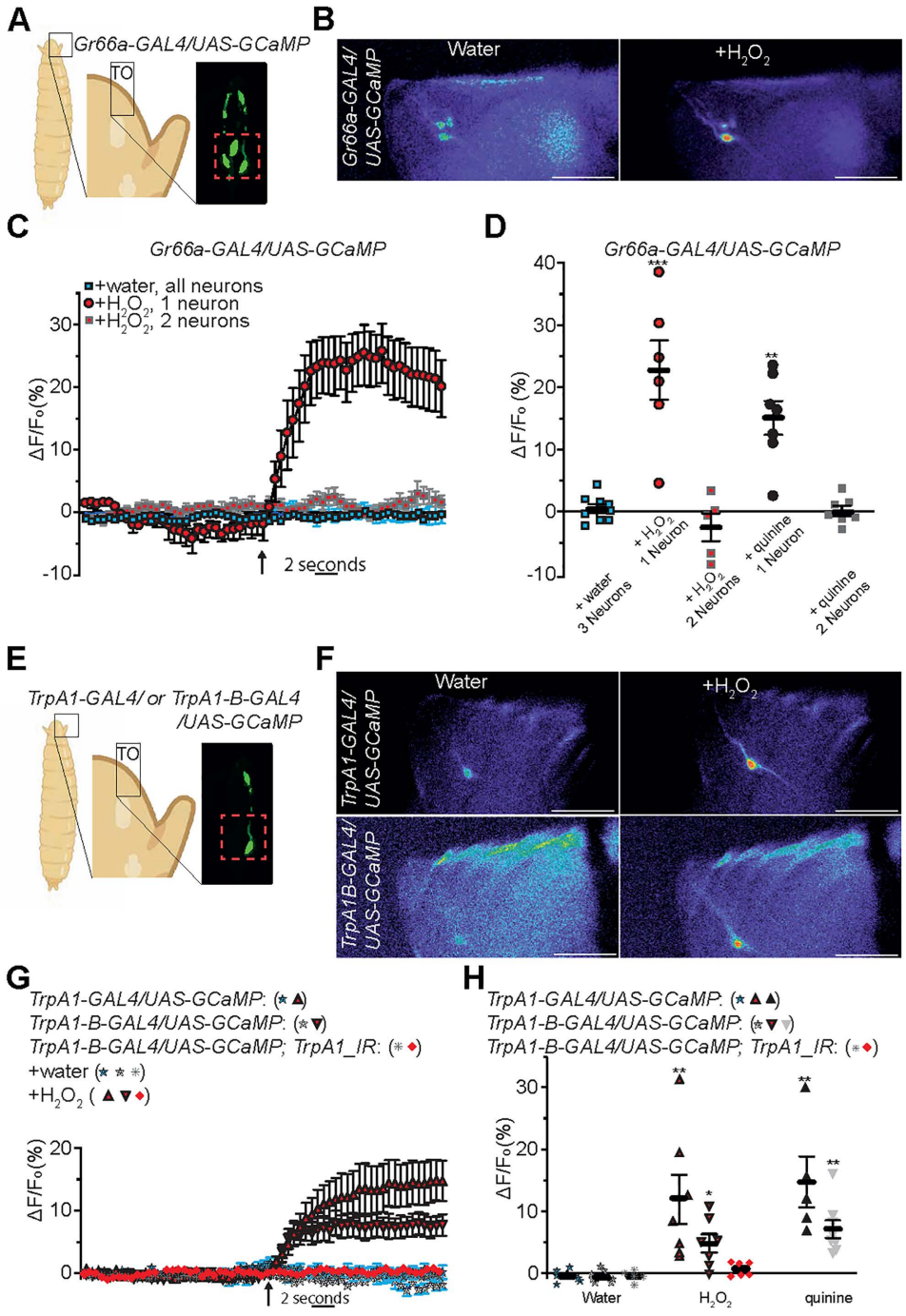



**Fig 5. The *TrpA1*+ neuron at the tip of the larval anterior part responds to $H_2O_2$ in a *TrpA1*-dependent manner. (A and E)** Graphical representation of larval region observed during the GCaMP assay with 3 neurons detectable without stimulation in *Gr66a-GAL4*/*UAS-GCaMP7s* animals (**A–D**) and 1 neuron detectable without stimulation in *TrpA1-GAL4*/*UAS-GCaMP7s* larvae as well as in *TrpA1-B-GAL4*/*UAS-GCaMP7s* animals **(E–H)**. **(B–D)** Addition of $H_2O_2$ triggers a calcium concentration increase in one out of the three *Gr66a*+ cells detectable in the anteriormost area of the larvae. **(B)** Representative images showing the GCaMP intensity before and after addition of either the control water or the $H_2O_2$ 1%. **(C)** Averaged ± SEM time course of the GCaMP intensity variations (ΔF/F0%) for *Gr66a*+ neurons. The addition of water ($n = 9$ flies) or $H_2O_2$ 1% ($n = 6$ flies) at a specific time is indicated by the arrow. **(D)** Averaged fluorescence intensity of negative peaks ± SEM in response to water ($n = 9$), $H_2O_2$ 1% ($n = 6$), or quinine (10 mM) ($n = 7$). **(E–H)** Addition of $H_2O_2$ triggers a calcium concentration increase in the unique *TrpA1*+ cell detectable in the anteriormost area of the larvae.

**(F)** Representative images showing the GCaMP intensity before and after addition of either the control water or the $H_2O_2$ 1%. **(G)** Averaged ± SEM time course of the GCaMP intensity variations (Δ*F*/*F*0%) for *TrpA1+* as well as *TrpA1-B+* neurons and *TrpA1-B* cells expressing *UAS-TrpA1_IR* (*TrpA1-B-GAL4/UAS-GCaMP7s; TrpA1_IR*). The addition of water ($n = 5–7$ flies) or $H_2O_2$ 1% ($n = 6–7$ flies) at a specific time is indicated by the arrow. **(H)** Averaged fluorescence intensity of negative peaks ± SEM in response to water ($n = 5–7$ flies), $H_2O_2$ 1% ($n = 6–7$ flies), or quinine (10 mM) ($n = 5–8$ flies). Scale bar is 20 μm. * Indicates $p = 0.0132$, ** indicates $p \leq 0.0098$, *** indicates $p \leq 0.009$, Kruskal–Wallis H test was used and the reference for a given assay is the same genotype exposed to water. Further details can be found in the detailed lines, conditions and, statistics for the figure section. The data underlying this Figure can be found in S1 Data. Created in BioRender. Kurz, L. (2026). https://core.local.biorender.dev/api/short-link/9ojribp.

https://doi.org/10.1371/journal.pbio.3004042.g005

abdominal coloration after ingestion (Fig 7A and 7B). Control ($w^-$) females do not discriminate between food sources when 1 mM sucrose is associated with a blue or red dye (preference index: P.I. = 0.5), flies with purple abdomen were observed (Fig 7B and 7C). However, animals robustly preferred 1 mM sucrose over a sucrose + PGN mixture, displaying a strong preference index for sucrose alone (P.I. > 0.8) (Fig 7C). To determine whether larval microbial experience was required for the emergence of this adult PGN avoidance, we tested flies raised on antibiotics throughout the larval stage. These individuals showed a markedly reduced avoidance of sucrose+PGN (P.I. < 0.55), with most animals ingesting both solutions. Finally, to evaluate the contribution of TrpA1—as anticipated from our PER results—we tested *TrpA1-KO* flies. These mutants consumed sucrose and sucrose+PGN equally, resulting in a strongly diminished preference index toward sucrose alone (P.I. = 0.51) (Fig 7C). Finally, the *TrpA1-BCE-KO* animals did not distinguish sucrose alone from the sucrose mixed with PGN (P.I. = 0.51) while *AD-KO* did make a discrimination, indicating that *-A* and *-D* isoforms are dispensable and suggesting *−B* and/or *−C* and/or *−E* as necessary.

Together, these results demonstrate that adult female flies avoid ingesting sucrose + PGN mixtures even under free-feeding conditions and that this avoidance requires prior larval cohabitation with bacteria. Moreover, TrpA1 appears to be crucial in limiting PGN ingestion, probably due to its role in the sensory priming that occurs during larval microbial exposure.

## Discussion

Our previous work demonstrated that certain bacteria have the ability to *prime Drosophila* larvae, leading to the emergence of adults whose gustatory system perceives bacterial PGN as an aversive molecule [37]. The objective of the present study was 2-fold: first, to identify the bacterial molecules capable of inducing this phenomenon, and second, to characterize the host proteins and cells through which the signal is received and transmitted.

The observation that two bacterial strains differing only in their ability to secrete uracil exhibit distinct priming properties highlights the crucial role of uracil in this process. Interestingly, the same metabolite appears to participate in several mechanisms underlying interactions between pathogenic bacteria and their hosts [41,43,44,55]. A more systematic analysis of the correlation between uracil production capacity and priming ability will help strengthen this finding and may reveal alternative priming mechanisms. Nonetheless, the fact that simple supplementation of the growth medium with uracil is sufficient to prime axenic larvae demonstrates that this bacterial signal is not only necessary but also sufficient to trigger the response. In this context, it will be important to determine the environmental factors that regulate and modulate bacterial uracil production.

Having identified ROS as the secondary messenger, we next asked which receptor and cell types are responsible for sensing and transmitting this signal. Using genetic tools enabling expression of specific TrpA1 isoforms, we identified a single neuronal cell located in the TO of the anterior extremity, co-expressing the TrpA1-B isoform and the Gr66a protein, as essential for priming. Selective inactivation of *TrpA1* in this neuron completely abolishes priming by bacteria that otherwise induce it in wild-type larvae. Moreover, expression of the *TrpA1-B* isoform—but not *TrpA1-A*—in this neuron alone is sufficient to rescue the phenotype of a pan-*TrpA1* mutant, indicating that the different isoforms differ in their ability to respond to ROS, as previously shown for other ligands such as heat or citronella. Our data therefore suggest that

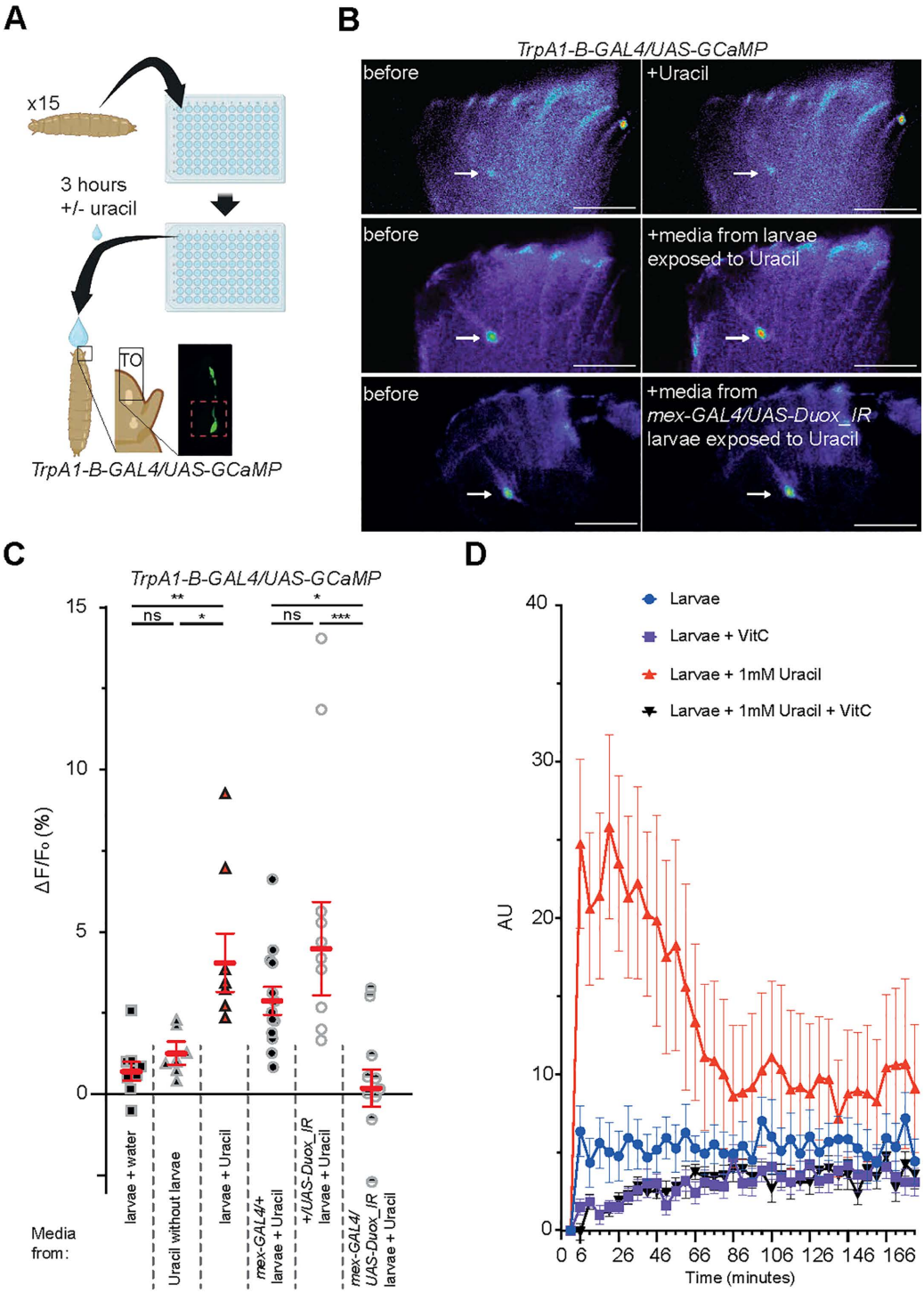



**Fig 6. The *TrpA1-B+* neuron responds to medium conditioned by larvae exposed to uracil. (A)** Graphical representation of the experimental design for the larva-conditioned medium. Fifteen larvae previously raised on antibiotic-containing medium are transferred at the L3 stage in a well containing either 100 μL of water or 100 μL of 1mM uracil diluted in water for 3 hours. After 3 hours in the dark at 25 °C, 50 μL of the medium in which the larvae were incubated is tested for its ability to trigger a calcium rise in the anterior part of *TrpA1-B-GAL4/UAS-GCaMP7s* larvae, which we consider naïve since they were raised on antibiotics and were not previously exposed to the larva-conditioned medium or to any of the chemicals tested. **(B)** Representative images showing the GCaMP intensity in the anteriormost *TrpA1-B+* neuron before and after addition of 50 μL of the medium: uracil alone or media form $w^-$ larvae exposed 3h to uracil or media form *mex-GAL4/UAS-Duox_IR* larvae exposed 3h to uracil. **(C)** Averaged fluorescence intensity of negative peaks ± SEM int the *TrpA1-B+* anteriormost neuron in response to either the chemicals used in the conditioned media assay (water, uracil) or

the medium in which the larvae were incubated in (media form $w^-$ larvae+water, media form $w^-$ larvae+uracil 1mM, media form *mex-GAL4*/+larvae+uracil 1mM, media form +/*UAS-Duox_IR*+uracil 1mM, media form *mex-GAL4*/*UAS-Duox_IR*+uracil 1mM). Each symbol represents a tested larva. **(D)** ROS are produced by larvae following exposure to uracil. L3 larvae were exposed to uracil and the presence of ROS was assayed within the wells over time. To confirm that ROS are the detected chemicals, Vitamin C (VitC) was applied to the samples. Scale bar is 20 μm. $*p < 0.05$, $**p \leq 0.0012$, $***p \leq 0.0002$. Statistical analyses were performed using the Kruskal–Wallis test for assays involving $w^-$ animals (non-normal distributions) and one-way ANOVA followed by Tukey's multiple-comparisons test for assays involving GAL4/UAS lines (after confirmation of normality). Further details can be found in the detailed lines, conditions and, statistics for the figure section. The data underlying this Figure can be found in S1 Data. Created in BioRender. Kurz, L. (2026). https://core.local.biorender.dev/api/short-link/9ojribp.

https://doi.org/10.1371/journal.pbio.3004042.g006

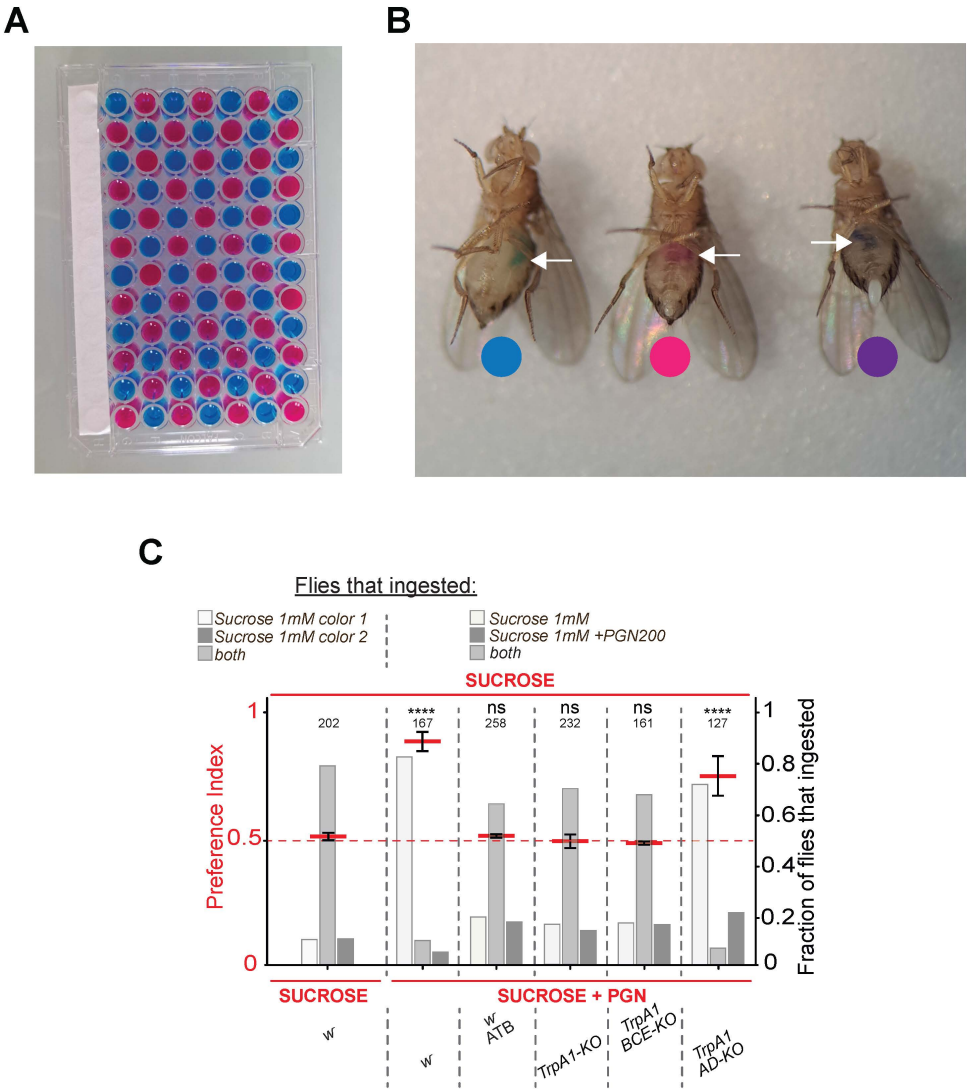



**Fig 7. PGN is avoided by free-moving animals in a 2-choices assay. (A–C)** Larval cohabitation with bacteria and the TrpA1 channel are necessary for a PGN-triggered aversion in a 2-choices assay. **(A)** The plates with the dye and (**B**) the flies that ingested the colored media leading to (**C**) the preference indexes for different conditions and genotypes as well as the fraction of flies that ingested the proposed mixtures. For **(C)**, the averaged preference index is in red with the standard error of the mean obtained from 6 to 8 independent experiments. The total amount of females tested is indicated on top of each assay. A preference index (PI) over 0.5 indicates a preference toward sucrose while a PI of 0.5 indicates either that two opposite behaviors occurred in the population or that a majority of animals consumed both solutions. The fraction of flies that ingested one, the other or both solutions allow to discriminate. In light colors are the fractions of flies that ingested one solution or both solutions. The animals from all the experiments were pooled for statistical analyses. ns indicates $p > 0.05$, **** indicates $p < 0.0001$ Chi-squared Test. Further details can be found in the material and methods section and in the source data file. The data underlying this Figure can be found in S1 Data.

https://doi.org/10.1371/journal.pbio.3004042.g007

bacterially derived uracil triggers Duox-dependent ROS production in the gut, which in turn activates TrpA1. Since *TrpA1* is also expressed in enteroendocrine cells, these were initially considered to be plausible mediators of ROS effects. However, our genetic analyses rule out this hypothesis and demonstrate that the *TrpA1*+/*Gr66a*+ neuron in the TO is required.

Our results suggest that uracil acts through the ROS production system, with this step taking place in the digestive tract. Indeed, in the absence of Duox activity specifically in the gut, bacteria lose their ability to prime larvae. The observation that a similar blockage occurs upon overexpression of catalase under the *mex-GAL4* promoter supports the idea that ROS must be generated in the gut, and further suggests that hydrogen peroxide is the main ROS involved.

Importantly, we demonstrated that uracil exposure increases ROS levels in larvae, further supporting a link between Duox activation and the priming response. Although several lines of evidence indicate that ROS are required for this process, our supplementation experiments suggest that ROS alone may not be sufficient to trigger priming. Whereas dietary uracil consistently induced the phenotype, exogenous $H_2O_2$ failed to do so, even after testing several concentrations and exposure regimens. Because exposure to 5% $H_2O_2$ caused detrimental effects, we subsequently tested lower concentrations (1%, 2%, and two successive exposures to 1% separated by 24 h), but none reproduced the effect of uracil.

One possibility would be that our supplementation protocol does not fully recapitulate the highly localized and transient production of ROS that occurs within the intestinal lumen following uracil sensing and Duox activation. Global exposure of the larvae to ROS could have detrimental effects that interfere with priming. Beyond this spatial constraint, it could be that ROS themselves may not constitute the biologically relevant signal. Instead, locally generated ROS could promote the oxidation of lipids or other biomolecules present in the gut lumen, leading to the formation of secondary metabolites such as reactive electrophilic metabolites. In vertebrates, lipid peroxidation-derived aldehydes, such as 4-hydroxynonenal (4-HNE), activate TRPA1 and contribute to physiological responses to oxidative stress [56]. More generally, TRPA1 channels are activated by a broad range of reactive electrophiles through covalent modification of conserved cysteine residues [57] and are now recognized as sensors of oxidative stress and tissue damage [58,59]. Although this mechanism has not yet been demonstrated in the *Drosophila* intestine, it provides an attractive explanation for our observations. Uracil-induced Duox activation could generate secondary electrophilic metabolites specifically within the intestinal lumen. Such metabolites would not necessarily be produced following dietary $H_2O_2$ supplementation, even if ROS levels were increased, thereby explaining why exogenous $H_2O_2$ fails to phenocopy uracil exposure.

This raises the question of the mechanistic link between ROS produced in the gut and activation of the TO neuron. One possibility is that ROS diffuse directly across the gut wall to reach the target neuron; however, this seems unlikely given the presence of enzymatic systems that rapidly degrade ROS. Alternatively, intermediate signaling steps could exist between intestinal ROS production and TrpA1 activation, implying that ROS are not the direct ligands of TrpA1 in the neuron as mentioned above. Our new results support a third, non–mutually exclusive mechanism in which ROS generated in the gut are released into the external environment and subsequently sensed by the anteriormost TrpA1-B+ neuron. We show that larvae exposed to uracil produce a Duox-dependent signal capable of activating TrpA1-B+ neurons in naïve individuals, as evidenced by calcium responses elicited by conditioned medium from uracil-treated larvae. Importantly, this activity is abolished when Duox is specifically knocked down in enterocytes of the donor larvae, indicating that intestinal Duox activity is required for generation of the signal. These findings suggest that a diffusible molecule—likely a ROS such as $H_2O_2$ or a derivative—is released from the gut and can act at a distance to activate TrpA1-B+ neurons. Such a mechanism implies that gut-derived ROS can function as inter-individual cues, potentially allowing infected larvae to transmit information about microbial presence to nearby conspecifics and thereby influence population-level behavior.

A central unresolved question is how microbial information acquired during the larval stage is transmitted across metamorphosis to shape adult sensory and behavioral outputs. This transition involves extensive tissue remodeling, including the destruction and reprogramming of larval structures, cycles of dedifferentiation and redifferentiation, and profound reorganization of neuronal circuits and epigenetic landscapes. Despite this dramatic rewiring, larval microbial exposure can lead to stable alterations in adult gustatory responses, suggesting the existence of persistent or re-encoded traces of early-life experience.

One possibility is that such information is maintained at the level of defined neural circuits. In this context, the TrpA1-B+ neuron emerges as a key candidate node linking microbial sensing to downstream behavioral adaptation. However, whether this neuron acts in isolation or as part of a broader network remains unclear. Sensory responses to bacterial cues in *Drosophila* are typically encoded by distributed circuits integrating gustatory, nociceptive, and neuromodulatory inputs. Mapping approaches such as GRASP or *trans*-Tango could therefore be used to identify synaptic partners of TrpA1-B+ cells and determine whether larval microbial experience reshapes a localized pathway or a distributed network. Such circuit-level analyses would clarify whether "priming" reflects a modification of a single sensory node or of a larger integrative circuit controlling adult aversion and feeding decisions.

Beyond circuit persistence, larval experience may also be encoded through transient functional states that are later re-established in the adult nervous system. Although metamorphosis involves the elimination or remodeling of many larval neurons, some peripheral and central gustatory neurons are known to persist or be re-specified, raising the possibility of partial continuity in sensory representations. However, given that adult proboscis responses rely on de novo sensory structures, a purely structural continuity model appears insufficient.

In parallel, more stable forms of information storage may also contribute to the persistence of larval experience across metamorphosis. Transcriptional reprogramming during development is extensive, yet certain neuronal populations retain conserved expression signatures or undergo tightly regulated fate transitions. Similarly, epigenetic mechanisms involving histone modifications and chromatin remodeling have been implicated in long-term developmental memory and could provide a substrate for encoding microbial history in specific neuronal subsets. Such mechanisms may be particularly relevant in restricted populations such as *Gr66a*− or *ppk23*-expressing neurons, which are known to participate in both larval and adult chemosensory circuits.

Finally, it is also possible that larval microbial exposure induces a form of distributed or associative-like memory that is not stored in a single neuronal substrate but instead emerges from coordinated changes across multiple levels of organization, including synaptic connectivity, transcriptional state, and epigenetic regulation.

Together, these hypotheses are not mutually exclusive. The most parsimonious model is likely one in which Duox-dependent ROS signaling initiates the formation of local electrophilic metabolites that act on sensory pathways, while parallel circuit-level and epigenetic mechanisms stabilize the resulting state across metamorphosis.

## Materials and methods

### Fly stocks

The reference strain in this study corresponds to *w1118* ($w^-$) BL#5905, *mex-GAL4* BL#91367, *UAS-Duox_IR* BL#38907, *mex-GAL4; TubG80ts* (this study and [60]; *TubG80ts* is BL#7016), *UAS-Catalase* BL#24621, *TrpA1-KO*/ *BCE-KO*/ *AD-KO*/ *BC-KO*/ *E-KO*/ *A-KI*/ *B-KI*/ *C-KI*/ *D-KI*/ *E-KI*, *TrpA1-GAL4*/ *A-GAL4*/ *B-GAL4*/ *C-GAL4*/ *E-GAL4* (all TrpA1 genetic tools were very kind gift from the Xiang lab with a lot of support and advices [45]), *UAS-GFP6x* BL#52262, *TrpA1-B-GAL4, UAS-GFP6x* (this study), *Gr66a-LexA; LexAop-mCherry* (gift from Zhang lab [61]), *UAS-TrpA1-IR* BL#36780, *Gr39a.b-GAL4* BL#57632, *Gr66a-GAL4* BL#28801, *TubG80ts; UAS-TrpA1_IR* (this study), *UAS-TrpA1-B; TrpA1*$^-$ (this study), *UAS-TrpA1-A; TrpA1*$^-$ (this study), *Gr66-GAL4; TrpA1*$^-$ (this study), *UAS-GCaMP7s* (gift from Matthieu Cavey), *UAS-GCaMP7s; UAS-TrpA1_IR* (this study) and *Gr66a-LexA, lexAop-GAL80; ppk23-GAL4* (gift form the Gordon lab).

### Fly culture

Flies were grown at 25 °C on a yeast/cornmeal medium in 12 h/12 h light/dark cycle-controlled incubators. For 1 L of food, 8.2 g of agar (VWR, cat. #20768.361), 80 g of cornmeal flour (Westhove, Farigel maize H1), and 80 g of yeast extract (VWR, cat. #24979.413) were cooked for 10 min in boiling water. 5.2 g of Methylparaben sodium salt (MERCK, cat. #106756) and 4 mL of 99% propionic acid (CARLOERBA, cat. #409553) were added when the food had cooled down. It is important to mention that our conventional media allows the presence of several bacterial species [37] and is

a protein-rich and sugar-poor culture medium. For germ-free condition, we raised flies on antibiotic (ATB) media. A mix of four ATB is added to the conventional media: Kanamycin + Tetracycline + Ampicillin + Erythromycin. For the experiments with Vitamin C and $H_2O_2$, we add 200 μL of Vitamin C at 0. 2 mg/mL on eggs laid for 6 hours on conventional media and 200 μL of $H_2O_2$ 1% on eggs laid for 6 hours on ATB media. We use a protein-rich rearing media, in contrast to the sugar-rich media used in some other laboratories. Consequently, our animals may be more sensitive to low sucrose concentrations (1 mM) compared to flies raised on sugar-rich media. Therefore, assays using 1 mM sucrose may not yield reproducible results when performed with flies reared on sugar-rich media.

### Bacterial stocks

*Levilactobacillus brevis* (*L. brevis*) is a gift form François Leulier's Lab.

*Erwinia carotovora* subsp. *carotovora 15* (Ecc$^{15}$) [62], *Ecc$^{15}$pyrE::tn5* [41] *and Ecc$^{15}$ Δ4* [63] are gifts from Won-Jae Lee Lab.

### Bacterial culture

*Ecc* strains were grown on standard LB agar plates at 30 °C at least 18 hours and *L. brevis* was grown in MRS agar in anaerobic-like conditions at 37 °C for at least 48 hours. A single colony was used to prepare liquid cultures. *Ecc* strains were grown in 200mL LB media (Lennox, Sigma-Aldrich ref L3022 or L2897) at 30 °C with agitation and *L. brevis* was grown in 50 mL MRS liquid media (Sigma-Aldrich ref 69964 agar and 69966 broth) static at 37 °C in sealed 50 mL tubes for anaerobic conditions. After overnight growth, the cultures were centrifuged for 15 min at 4,200 rpm. Bacterial doses were adjusted by measuring culture turbidity at an optical density of 600 nm to set the culture to OD 1. For the heat kill experiment, we set the OD to 1 from an overnight-incubated culture, then incubate this sample at 95 °C for 5 min. We confirm the heat-kill experiment using an MRS agar plate containing the sample before and after heat kill. For the supernatant experiment, we set the OD to 1 from an overnight-incubated culture, then centrifuged and the supernatant is then filtered with a 0.45 μm filter.

### Proboscis Extension Reflex (PER) behavior

All flies used for the test were females between 5 and 7 days old. Unless experimental conditions require it, the flies are kept and staged at 25 °C to avoid any temperature changes once they are put into starvation. The day before, the tested flies are starved in an empty tube with water-soaked plug for 24 h at 25 °C. Eighteen flies are tested in one assay, 6 flies are mounted on one slide and in pairs under each coverslip. To prepare the slide, three pieces of double-sided tape are regularly spaced on a slide. Two spacers are created on the sides of each piece of tape by shaping two thin cylinders of UHT paste. To avoid the use of carbon dioxide flies are anesthetized on ice. Under the microscope, two flies are stuck on their backs, side by side, on same piece of tape so that their wings adhere to the tape. A coverslip is then placed on top of the two flies and pressed onto the UHT paste, blocking their front legs and immobilizing them. Once all slides are prepared, they are transferred to a humid chamber and kept at 25 °C for 1.5 h to allow the flies to recover before the assay. Flies are tested in pairs, the test is carried out until completion on a pair of flies (under the same coverslip), and then move on to the next pair. Before the test, water is given to each pair of flies to ensure that the flies are not thirsty and do not respond with a PER to the water in which the solutions are prepared. Stimulation with the test solution is always preceded and followed by a control stimulation with a sweet solution, to assess the fly's condition and its suitability for the test. During the test small strips of filter paper are soaked in the test solution and used to contact the fly's labellum (three consecutive times per control and test phase). Contact with the fly's proboscis should be as gentle as possible. Ideally, the head should not move. A stronger touch may prevent the fly from responding to subsequent stimulation. Based on the protocol needed the test is done following the sequence and the timing in the Table 1 below.

**Table 1. Aversion protocol.**

| | | | | | | | | | | |
|---|---|---|---|---|---|---|---|---|---|---|
| Water to satiety | Wait 1 min | CONTROL Sucrose 1 mM Repeated 3 times | Wait 1 min | Water one time | Wait 1 min | TEST Repeated 3 times | Wait 1 min | Water one time | Wait 1 min | CONTROL Sucrose 1 mM Repeated 3 times |

https://doi.org/10.1371/journal.pbio.3004042.t001

All solutions to be tested are prepared the test day and stored at room temperature. In the aversion protocol, the control stimulation is performed with 1 mM sucrose (D(+)-sucrose ≥99.5%, p.a. Carl Roth GmbH + Co. KG). This concentration is sufficient to elicit a PER but is not so high as to influence the response to the subsequent test stimulation. PGN is *E. coli* K12: Invivogen, catalog code #tlrl-kipgn. After each control or test stimulation, a water-soaked strip is used to tap the proboscis and clean it. The response of each fly to each stimulation is recorded. We distinguish between two types of flies: those able to respond and those unable to respond. To make this distinction, we use three control stimulations before the test and three after the test. Flies that do not respond during the control stimulations (1 mM sucrose) are classified as "unable to respond" and are excluded from the analysis, regardless of their responses during the tests. Flies that respond during the control stimulations are classified as "able to respond," and only their responses during the tests are included in the statistical analyses. Consequently, each fly 'able to respond' is attributed a 0 when it does not extend the proboscis toward the tested solution while it is attributed a 1 when it extends the proboscis toward the tested solution. Each fly represents an independent observation and the PER index is calculated as the percentage of flies tested that responded with a PER to the TEST stimulation and represented with the ± 95% confidence Interval (CI). For instance, if out of 30 tested animals, 21 extended their proboscis toward the tested solution, the PER index will be of 0.7. As the values obtained from one fly are categorical data with a *Yes* or *No* value, we used the Fisher's exact test and the 95% CI to test the statistical significance of a possible difference between a test sample and the related control. This test takes into account the response of each fly and does not simply compare the distribution of several values without taking into account the size of the cohort used to generate this value. For PER assays, at least 3 independent experiments involving up to 18 flies each were performed. The results from all the flies were gathered and the total amount of animals tested is indicated in the graph. In addition, we do not show the average response from one experiment representative of the different biological replicates, but the PER index from all the tested animals in one graph. While several independent batches of flies are tested, the final PER index includes all the flies and the PER index of each independent batch is also shown as open dots in the graphs to illustrate the variability. In case of stage-dependent experiments, flies are shifted from one condition to another upon hatching.

### Monoassociation

An oviposition of $w^-$ germ-free flies is set up on an apple agar plate with yeast at 25 °C for 6 hours. Three petri dishes are filled with 2.6% bleach, 70% ethanol (Ethanol 96° RPE Carlo Erba Ref 414638) and autoclaved purified distilled water, respectively. The embryos are collected by filling the plate in which oviposition occurred with purified distilled water and using a small brush to gently detach them from the flies' food. A 40 μm cell strainer is used to collect the embryos. The cell strainer with the embryos is then dipped into: bleach 2.6% for 5 min, ethanol 70% for 1 min, purified water for 1 min, ethanol 70% for 1 min, purified water for 1 min. The brush used to collect the embryos is sterilized in 2.6% bleach for 10 min, rinsed and then used to transfer the sterile embryos onto the desired media.

We then deposit bleach eggs on 'steril' conventional media (medium is deposited in sterilized Falcon tubes in sterile conditions and sealed with a cap) and add 200 μL of the monoassociation we want (MRS broth, MRS broth + *L. brevis* or supernatant or heat-killed bacteria, LB broth, LB broth + bacteria, LB broth + uracil, LB broth + thymine, LB broth + cytosine, LB brothy + $H_2O_2$).

### RNAi

All the tested animals were F1 obtained from a cross between parents possessing the *GAL4* transgene and parents possessing the *UAS-RNAi* construction or from crosses between $w^-$ animals (genetic background of the *GAL4* and *UAS* lines) and a transgenic line to serve as ctrl.

For stage-dependent RNAi experiments, the ubiquitously expressed *Tub-GAL80$^{ts}$*, that inhibits the activity of *GAL4*, is temperature sensitive: it's active at 18 °C and inactivated at 29 °C, allowing the expression of *UAS* when animals are raised at 29 °C and preventing it at 18 °C. For RNAi in larvae only, animals were raised from eggs to early pupae at 29 °C and then shifted at 18 °C. for RNAi in adults only, eggs, larvae and pupae were raised at 18 °C and the virgin adults shifted to 29 °C.

### Larval-conditioned medium

Conditioned medium was used to highlight signals such as ROS produced by enterocytes in response to 1 mM uracil to potentially activate the *TrpA1-B+* neuron. In a 96-well plate (NUNC), conditioned medium was obtained by placing 15 larvae of adequate genotype, reared on antibiotic-containing medium, in a well containing either 100 µL of water or 100 µL of 1mM uracil diluted in water for 3 hours. Fifty microliters of conditioned medium was then tested on the anterior part of *TrpA1-GAL4*/*UAS-GCaMP7s* larva reared on normal food in calcium imaging experiments. 100 µL of 1mM uracil was also placed in a well without any larvae during 3 hours to test the activity of 1mM uracil on the *TrpA1-B+* neuron localized in the terminal organ of *TrpA1-GAL4*/*UAS-GCaMP7s* larva.

### Reactive oxygen species measurement in first-stage larvae

Thirty L1 larvae were collected from 24-hours monoassociation tubes containing either LB or LB supplemented with 1 mM uracil. Samples were homogenized and centrifuged. ROS levels were quantified using the Amplex Red Hydrogen Peroxide/Peroxidase Assay Kit (Invitrogen, #A12222), as previously described [64]. Briefly, 20 µL of sample was mixed with 100 µL of reaction buffer containing 50 µM Amplex Red reagent and 0.2 U/mL horseradish peroxidase. Fluorescence intensity was measured using a CLARIOstar Plus microplate reader (BMG Labtech) with excitation at 545 nm (±15 nm) and emission at 590 nm (±8 nm). A standard curve was generated using serial dilutions of $H_2O_2$ and used to calculate $H_2O_2$ concentrations in the samples.

### Reactive oxygen species measurement over time in third-stage larvae

Reactive oxygen species (ROS) levels in the larval medium were detected using the L-012 chemiluminescent probe (Merck-Sigma-Aldrich). Before assays, 15 third-instar larvae were placed in 100 µL of PBS per well in a 96-well Microfluor 1 black plate (Thermo Scientific) and 8 wells of 15 larvae were used per condition. 8 additional wells containing PBS without larvae were used as background control. The experiment was repeated twice. To initiate the experiment, the PBS was replaced with either 100 µL of PBS alone (control), 100 µL of PBS supplemented with ascorbic acid (20 µg/mL), 100 µL of PBS supplemented with uracil (1 mM), or 100 µL of PBS supplemented with uracil (1 mM) and ascorbic acid (20 µg/mL). L-012 was added at a final concentration of 200 µM in all wells.

Chemiluminescence was measured every 5 min during 3 h using an Infinite M200Pro microplate reader (TECAN) with an integration time of 3 s per well at room temperature in the dark. ROS levels were expressed as relative luminescence units (RLU). At the end of the experiment, $H_2O_2$ was added to each well at final concentration of 1 mM to verify that L-012 had not been depleted during the experiment. Background luminescence values were subtracted to luminescence values detected in wells containing larvae.

### Choice assay

Two-way choice assays were performed essentially as described [65]. Briefly, 5- to 7-day-old female flies (30 ± 10 flies per experiment) were starved for ~18 h at 25 °C and placed into a 96-well plate with 1% agarose in each well. Alternating

wells contained either red (sulforhodamine B, 0.2 mg/mL; Sigma-Aldrich) or blue dye (bleu E133 meilleur du chef, 0.3%). Then we deposit 10 μL of solution containing sucrose 1mM or Sucrose1mM + PGN 200 μg/ml on top of the well. Each experiment is carried out in duplicate by placing the components on two different colors (*e.g.*, sucrose 1mM on blue wells for plate A and on red wells for plate B) to verify whether there is an effect of color. The flies were allowed to feed in the dark for 90 min at ~23 °C. We transferred the plates to −20 °C for 15 min in order to rapidly freeze the flies in order to count the flies based on their abdominal color under a binocular microscope. The numbers of flies with blue, red, or purple (mixed red and blue) abdomens were tabulated (Fig 7A and 7B), and the P.I. was determined: $(N_{suc} + 0.5N_{mix})/(N_{suc} + N_{test} + N_{mix})$. The flies without colors in their abdomen were discarded. The number of flies indicated corresponds to animals with colored abdomens.

### Microscopy

No immunostaining was performed. To image larvae sensory organs and body as well as gut and brains, full larvae were killed with heat and mounted whole on slides using Vectashield fluorescent mounting medium. Organs were dissected in PBS, rinsed with PBS and directly mounted on slides using Vectashield fluorescent mounting medium. The tissues were visualized directly after. Images were captured with LSM 780 Zeiss confocal microscope (20× air objective was used). Images were processed using Adobe Photoshop and FiJi softwares.

### Statistics

GraphPad Prism 8 software was used for statistical analyses. For in vivo calcium imaging, the D'Agostino–Pearson test to assay whether the values are distributed normally was applied. As not all the data sets were considered normal, non-parametric statistical analysis such as Kruskal–Wallis *H* test was used for all the data presented. For PER datasets, each fly 'able to respond' is attributed a 0 when it does not extend the proboscis toward the tested solution while it is attributed a 1 when it extends the proboscis toward the tested solution. As the values obtained from one fly are categorical data with a *Yes* or *No* value, we used the Fisher's exact test and the 95% CI to test the statistical significance of a possible difference between a test sample and the related control. This test takes into account the response of each fly and does not simply compare the distribution of several values without taking into account the size of the cohort used to generate this value. For PER assays, at least 3 independent experiments involving up to 18 flies each were performed. The results from all the flies were gathered and the total amount of animals tested is indicated in the graph. In addition, we do not show the average response from one experiment representative of the different biological replicates, but the PER index from all the tested animals in one graph. Each fly represents an independent observation and the PER index is calculated as the percentage of flies tested that responded with a PER to the TEST stimulation and represented with the ± 95% CI. For instance, if out of 30 tested animals, 21 extended their proboscis toward the tested solution, the PER index will be of 0.7. Several independent batches of flies are tested, the final PER index includes all the flies and the PER index of each independent batch is also shown as open dots in the graphs to illustrate the variability.

### Chemicals

PGN-ECndi ultrapure peptidoglycan catalog code #tlrl-kipgn InvivoGen USA, D (+)-Saccharose ≥99.5%.ref 4621.1 Carl Roth, $H_2O_2$ solution ref. H3410 (Figs 1 and 5) and H1009 (S5 Fig) Sigma-Aldrich, Acid L-ascorbic (Vitamin C) ref. A92902 Sigma-Aldrich, Uracil ≥99.0%. refU0750 Sigmal-Aldrich, Cytosine ≥99.0%. refC3506 Sigmal-Aldrich, Thymine ≥99.0%. refT0376 Sigmal-Aldrich Quinine ref. Q1125 Sigma-Aldrich and Catalase ref.C40 Sigmal-Aldrich.

### Calcium imaging experiments

In vivo larval calcium imaging experiments were performed on beginning of third-instar larvae. Larvae were immobilized in a small drop of distilled water placed between two plastic coverslips (22 mm × 22 mm, Agar Scientific). The two coverslips

were held together to prevent movement of the anterior part of the larva using an alligator clip attached to a support. Stimulation was performed manually using a pipette with gel-loading tip by applying water, Uracil (1 mM) diluted in water, $H_2O_2$ (1%), quinine (10 mM, Sigma-Aldrich #Q11125) diluted in water or 50 μL conditioned medium through a hole made in the upper coverslip allowing the solutions to come into contact with the larval TO. For larval calcium imaging experiments, GCaMP7s was excited using a Lumencor diode light source at 482 nm ± 25. Emitted light was collected through a 505–530 nm band-pass filter. Images were collected every 500 ms using a Hamamatsu/HPF-ORCA Flash 4.0 camera and processed using Leica MM AF 2.2.9. Each experiment consisted of a recording of 70–100 images before stimulation and 160 images after stimulation. Data were analyzed as previously described [31] by using FIJI (https://fiji.sc/). For larvae fluorescence quantifications, a background fluorescence variation was calculated and subtracted to the fluorescence variation signal.

### Detailed lines, conditions and statistics for the figure section

All these data are downloadable with the source data file.

Graphical abstract and some icons were created in BioRender (https://www.biorender.com/) under an institutional license (Aix-Marseille Université).

## Supporting information

**S1 Fig. Priming model: Larval exposure to bacteria is mandatory.** (**A**) Graphical representation of the priming model: adults derived from larvae raised without bacterial cohabitation do not reject sucrose + PGN mixtures. In contrast, adults from larvae cohabiting with bacteria in conventional media are attracted to sucrose but reject sucrose + PGN, a response dependent on larval *Gr66a*+ neurons with functional *TrpA1* and adult *ppk23*+ cells. (**B**) Graphical representation of the mono-association protocol used to expose larvae to a specific bacterial strain, followed by PER assay testing of the sucrose + PGN mixture in the resulting adults. Eggs are sterilized with bleach and deposited on a freshly made conventional media poured in a sterile culture tube and sealed with an autoclaved plug. Selected chemicals such as LB or LB + uracil are added on top of the eggs, same with bacteria. Created in BioRender. Kurz, L. (2026). https://core.local.biorender.dev/api/short-link/9ojribp.
(TIF)

**S2 Fig. Larval exposure to thymine does not prime.** Uracil 20 nM or thymine 1 mM are not sufficient to prime the larvae. Sterilized eggs were exposed to the different treatments and the resulting adults raised on antibiotics-containing media (ATB). Specifically, eggs were exposed to LB media containing uracil or thymine. PER index of $w^-$ flies to control solutions of sucrose and sucrose + PGN from *E. coli* K12 at 200 μg/mL (PGN200) was obtained. The semi-transparent data are shown for reference and correspond to related control and test data presented in Fig 1B. The PER index is calculated as the percentage of flies tested that responded with a PER to the stimulation ± 95% confidence interval (CI). A PER value of 1 means that 100% of the tested flies extended their proboscis following contact with the mixture, a value of 0.2 means that 20% of the animals extended their proboscis. The number of tested flies (*n*) is indicated on top of each bar. For each condition, at least 3 groups with a minimum of 10 flies per group were used. Each independent group is represented as an open circle. ns indicates $p > 0.05$ Fisher's exact test. Further details can be found in the detailed lines, conditions and, statistics for the figure section. The data underlying this Figure can be found in S1 Data.
(TIF)

**S3 Fig. Larvae exposed to uracil give rise to PGN-responsive adults. *ppk23*+/*Gr66a*− neurons respond to stimulation with PGN on the labellum only when larvae were exposed to uracil.** Real-time calcium imaging using the calcium indicator GCaMP7s to reflect the in vivo neuronal activity of *ppk23*+/*Gr66a*− neurons (*Gr66a-LexA; LexAop GAL80; ppk23-GAL4*/*UAS-GCaMP7s*) in adult brains of flies whose proboscis has been stimulated with PGN. The expression of

*LexAop-GAL80* antagonizes the activity of GAL4, thus preventing the expression of GCaMP7S in *Gr66a+*/*ppk23+* neurons. (**A**) Representative images showing the GCaMP7s intensity before and after addition of either the control NaCl 100 mM or the peptidoglycan 200 μg/mL. (**B**) Averaged ± SEM time course of the GCaMP7s intensity variations (ΔF/F0%) for *ppk23+*/*Gr66a−* neurons. The addition of peptidoglycan at 200 μg/mL to adults obtained from larvae exposed to LB media ($n = 8$ flies) or adults obtained from larvae exposed to LB media + uracil ($n = 7$ flies) at a specific time is indicated by the arrow. (**C**) Averaged fluorescence intensity of negative peaks ± SEM for peptidoglycan- or NaCl-treated flies obtained from larvae exposed ($n = 7$) or not ($n = 8$) to LB media + uracil. ns indicates $p > 0.05$, ** indicates $p < 0.004$; non-parametric *t* test, two-tailed Mann–Whitney test. The data underlying this Figure can be found in S1 Data.
(TIF)

**S4 Fig. In larvae, the mex-*GAL4* driver is exclusively expressed in enterocytes.** (**A–C**) Confocal images of larvae expressing *gfp* under the control of the *mex-GAL4* driver. Shown are representative pictures of the anterior extremities (**A**), the brains (**B**) and the guts (**C**). In (**A–C**), the anterior is indicated with an asterisk.
(TIF)

**S5 Fig. Vitamin C at 0.2 mg/mL is not bactericidal and $H_2O_2$ 1% does not impair larval development.** (**A**) Vitamin C can be bactericidal. Vitamin C was added or not to a bacterial liquid culture and the OD 600 nm was measured 24 hours later following an incubation at 30 °C with agitation. ****$p = 0.056$, non-parametric *t* test, Mann–Whitney test. (**B**) $H_2O_2$ supplementation does not rescue the absence of priming on axenic media (ATB). $H_2O_2$ (reference H3410: used all over the study) and another chemical reference (H1009) were added to eggs laid on ATB-containing media. All the resulting adults were raised on antibiotics-containing media. PER index to solutions of sucrose + PGN (PGN200) of $w^-$ flies was obtained. The PER index is calculated as the percentage of flies tested that responded with a PER to the stimulation ± 95% confidence interval (CI). A PER value of 1 means that 100% of the tested flies extended their proboscis following contact with the mixture, a value of 0.2 means that 20% of the animals extended their proboscis. The number of tested flies (*n*) is indicated on top of the bar. At least 3 groups with a minimum of 10 flies per group were used. Each independent group is represented as an open circle. Further details can be found in the detailed lines, conditions and, statistics for the figure section. (**C**) $H_2O_2$ 1% (reference H3410) does not obviously impair larval growth. Images of tubes containing medium with antibiotics four days after bleached eggs deposition, followed immediately by addition of $H_2O_2$ at the indicated percentage. The data underlying this Figure can be found in S1 Data.
(TIF)

**S6 Fig. *TrpA1-C* and *TrpA1-E GAL4* drivers, but not *TrpA1-B-GAL4* are expressed in C4da neurons.** (**A** and **B**) Representative confocal images of larvae expressing *gfp* under the control of the *TrpA1-C-GAL4* driver (**A**) or the *TrpA1-E-GAL4* driver (**B**). Shown are the C4da neurons in the anterior extremity with a dorsal view (**A**) or a magnified lateral view of a single C4da cell (**B**). In panels (**A**) and (**B**), anterior is oriented to the left, and a schematic representation of the whole larva indicates the depicted area. Neurons with dendrites extending toward the external environment are indicated by (t). Created in BioRender. Kurz, L. (2026). https://core.local.biorender.dev/api/short-link/9ojribp.
(TIF)

**S7 Fig. *Gr66a+* cells are present in larval anterior, brain, but not in the gut.** (**A**–**C**) Representative confocal images of larvae expressing *gfp* under the control of the *Gr66a-GAL4* driver with the anterior extremity (**A**), the brain (**B**) and the gut (**C**). The anterior is either on the left (**A**) or indicated with an asterisk (**B** and **C**). Neurons with dendrites extending toward the external environment are indicated by (t) and despite being fainter dorsal pharyngeal sensilla ganglion (d) and ventral pharyngeal sensilla ganglion (v) are detectable. A schematic representation of the whole larva indicates the depicted area. Created in BioRender. Kurz, L. (2026). https://core.local.biorender.dev/api/short-link/9ojribp.
(TIF)

**S8 Fig. The TrpA1-A isoform is expressed according to an expression pattern that is different from that of the −B, −C and −E isoforms.** (**A**–**C**) Representative confocal images of larvae expressing *gfp* under the control of the *TrpA1-A-GAL4* driver with the anterior extremity (**A**), the brain (**B**) and the gut (**C**). The anterior is either on the left (**A**) or indicated with an asterisk (**B** and **C**). A schematic representation of the whole larva indicates the depicted area. Created in BioRender. Kurz, L. (2026). https://core.local.biorender.dev/api/short-link/9ojribp.
(TIF)

**S9 Fig. *Gr39a.b-GAL4* driver is only expressed in anterior neurons and includes *TrpA1-B*+ cell.** (**A–C**) Confocal images of larvae expressing *gfp* under the control of the *Gr39a.b-GAL4* driver (**A**), the *TrpA1-B-GAL4* driver as well as the *Gr39a.b-GAL4* driver (**B**). Shown are the anterior parts (**A–B**) and the guts (**C**). In (**A–C**), the anterior is on the left and the larger square is a magnification of the most anterior part of the animal housing neurons whose dendrites extend toward the external environment (t), a schematic representation of the whole larva indicates the depicted area. Created in BioRender. Kurz, L. (2026). https://core.local.biorender.dev/api/short-link/9ojribp.
(TIF)

**S10 Fig. Quinine triggers a calcium increase in one *Gr66a*+ neuron as well as in the anteriormost *TrpA1*+ *neuron.*** (**A** and **D**) Graphical representation of larval region observed during the GCaMP assay with 3 neurons detectable without stimulation in *Gr66a-GAL*/*UAS-GCaMP7s* animals (**A**–**C**) and 1 neuron detectable without stimulation in *TrpA1-GAL4*/*UAS-GCaMP7s* larvae as well as in *TrpA1-B-GAL4*/*UAS-GCaMP7s* animals (**D**–**F**). (**B** and **C**) Addition of quinine triggers a calcium concentration increase in one out of the three *Gr66a*+ cells detectable in the anteriormost area of the larvae. (**B**) Representative images showing the GCaMP intensity before and after addition of either the control water or the quinine (10 mM). (**C**) Averaged ± SEM time course of the GCaMP intensity variations (Δ*F*/*F*0%) for *Gr66a*+ neurons. The addition of water ($n = 9$ flies) or quinine ($n = 7$ flies) at a specific time is indicated by the arrow. (**D**–**F**) Addition of quinine triggers a calcium concentration increase in the unique *TrpA1*+cell detectable in the anteriormost area of the larvae. (**E**) Representative images showing the GCaMP intensity before and after addition of either the control water or the quinine. (**F**) Averaged ± SEM time course of the GCaMP intensity variations (Δ*F*/*F*0%) for *TrpA1*+ as well as *TrpA1-B*+ neurons. The addition of water ($n = 5$–8 flies) or quinine ($n = 5$–8 flies) at a specific time is indicated by the arrow. Scale bar is 20 μm. (**G**) Quinine 10 mM is not sufficient to prime the larvae. Sterilized eggs were exposed to quinine 10 mM and the resulting adults raised on antibiotics-containing media (ATB). Specifically, eggs were exposed to LB media containing quinine on monoassociation media. PER index of $w^-$ flies to control solutions of sucrose and sucrose + PGN from *E. coli* K12 at 200 μg/mL (PGN200) was obtained. The semi-transparent data are shown for reference and correspond to related control and test data presented in Fig 1B. The PER index is calculated as the percentage of flies tested that responded with a PER to the stimulation ± 95% confidence interval (CI). A PER value of 1 means that 100% of the tested flies extended their proboscis following contact with the mixture, a value of 0.2 means that 20% of the animals extended their proboscis. The number of tested flies (n) is indicated on top of each bar. For each condition, at least 3 groups with a minimum of 10 flies per group were used. Each independent group is represented as an open circle. ns indicates $p > 0.05$ Fisher's exact test. Further details can be found in the detailed lines, conditions and, statistics for the figure section. The data underlying this Figure can be found in S1 Data. Created in BioRender. Kurz, L. (2026) https://core.local.biorender.dev/api/short-link/9ojribp.
(TIF)

**S11 Fig. Time course response of the *TrpA1-B*+ neuron responding to medium conditioned by larvae exposed to uracil.** Averaged time course of the GCaMP intensity variations (Δ*F*/*F*0%) for *TrpA1-B*+ neurons (*TrpA1-B-GAL4*/*UAS-GCaMP7s*) in response to either the chemicals used in the conditioned media assay (uracil; $n = 7$) or the medium in which the larvae were incubated in (media form $w^-$ larvae + water ($n = 8$) or media form $w^-$ larvae + uracil 1mM ($n = 6$). The addition of the chemical or the conditioned media at a specific time is indicated by the arrow.
(TIF)

**S1 Data. Numerical data used in panels of the Figures and supplemental Figures.**
(XLSX)

## Acknowledgments

Annelise Vialat-Lieutaud, Serge Loquin, Amandine Chlémaire. We gratefully acknowledge the laboratory UMR 1347 Agroécologie (Dijon, France) for providing access to the materials, chemicals, and resources necessary for the time-course measurement of ROS in third-stage larvae.

## Author contributions

**Conceptualization:** Romane Milleville, Gerard Maniere, Julien Royet, Cyril Léopold Kurz.

**Data curation:** Romane Milleville, Gerard Maniere, Martine Berthelot-Grosjean, Olivier Lamotte, Cyril Léopold Kurz.

**Formal analysis:** Gerard Maniere, Martine Berthelot-Grosjean, Olivier Lamotte.

**Funding acquisition:** Yael Grosjean, Julien Royet.

**Investigation:** Romane Milleville.

**Methodology:** Romane Milleville.

**Project administration:** Yael Grosjean.

**Resources:** Julien Royet.

**Supervision:** Gerard Maniere, Julien Royet, Cyril Léopold Kurz.

**Writing – original draft:** Romane Milleville, Gerard Maniere, Julien Royet, Cyril Léopold Kurz.

**Writing – review & editing:** Julien Royet, Cyril Léopold Kurz.

## References

1. McFall-Ngai M, Hadfield MG, Bosch TCG, Carey HV, Domazet-Lošo T, Douglas AE, et al. Animals in a bacterial world, a new imperative for the life sciences. Proc Natl Acad Sci U S A. 2013;110(9):3229–36. https://doi.org/10.1073/pnas.1218525110 PMID: 23391737
2. Yu KB, Hsiao EY. Roles for the gut microbiota in regulating neuronal feeding circuits. J Clin Invest. 2021;131(10):e143772. https://doi.org/10.1172/JCI143772 PMID: 33998595
3. You H, Lee WJ, Lee W-J. Homeostasis between gut-associated microorganisms and the immune system in *Drosophila*. Curr Opin Immunol. 2014;30:48–53. https://doi.org/10.1016/j.coi.2014.06.006 PMID: 24997434
4. Nguyen B, Than A, Dinh H, Morimoto J, Ponton F. Parental microbiota modulates offspring development, body mass and fecundity in a polyphagous fruit fly. Microorganisms. 2020;8(9):1289. https://doi.org/10.3390/microorganisms8091289 PMID: 32846933
5. Gould AL, Zhang V, Lamberti L, Jones EW, Obadia B, Korasidis N, et al. Microbiome interactions shape host fitness. Proc Natl Acad Sci U S A. 2018;115(51):E11951–60. https://doi.org/10.1073/pnas.1809349115 PMID: 30510004
6. Little TJ, Hultmark D, Read AF. Invertebrate immunity and the limits of mechanistic immunology. Nat Immunol. 2005;6(7):651–4. https://doi.org/10.1038/ni1219 PMID: 15970937
7. Schwenke RA, Lazzaro BP, Wolfner MF. Reproduction–Immunity trade-offs in insects. Annu Rev Entomol. 2016;61(Volume 61):239–56. https://doi.org/10.1146/annurev-ento-010715-023924
8. Clark RI, Tan SWS, Péan CB, Roostalu U, Vivancos V, Bronda K, et al. MEF2 is an in vivo immune-metabolic switch. Cell. 2013;155(2):435–47. https://doi.org/10.1016/j.cell.2013.09.007 PMID: 24075010
9. Finlay BB, McFadden G. Anti-immunology: Evasion of the host immune system by bacterial and viral pathogens. Cell. 2006;124(4):767–82. https://doi.org/10.1016/j.cell.2006.01.034 PMID: 16497587
10. Flyg C, Kenne K, Boman HG. Insect pathogenic properties of *Serratia marcescens*: Phage-resistant mutants with a decreased resistance to Cecropia immunity and a decreased virulence to *Drosophila*. J Gen Microbiol. 1980;120(1):173–81. https://doi.org/10.1099/00221287-120-1-173 PMID: 7012273
11. Nehme NT, Liégeois S, Kele B, Giammarinaro P, Pradel E, Hoffmann JA, et al. A model of bacterial intestinal infections in *Drosophila melanogaster*. PLoS Pathog. 2007;3(11):e173. https://doi.org/10.1371/journal.ppat.0030173 PMID: 18039029
12. Kraus A, Buckley KM, Salinas I. Sensing the world and its dangers: An evolutionary perspective in neuroimmunology. Elife. 2021;10:e66706. https://doi.org/10.7554/eLife.66706 PMID: 33900197

13. Trabanelli S, Akselrod M, Fellrath J, Vanoni G, Bertoni T, Serino S, et al. Neural anticipation of virtual infection triggers an immune response. Nat Neurosci. 2025;28(9):1968–77. https://doi.org/10.1038/s41593-025-02008-y PMID: 40721674
14. Kacsoh BZ, Bozler J, Ramaswami M, Bosco G. Social communication of predator-induced changes in *Drosophila* behavior and germ line physiology. Elife. 2015;4:e07423. https://doi.org/10.7554/eLife.07423 PMID: 25970035
15. Masuzzo A, Montanari M, Kurz L, Royet J. How bacteria impact host nervous system and behaviors: Lessons from flies and worms. Trends Neurosci. 2020;43(12):998–1010. https://doi.org/10.1016/j.tins.2020.09.007 PMID: 33051027
16. Montanari M, Royet J. Impact of microorganisms and parasites on neuronally controlled *Drosophila* behaviours. Cells. 2021;10(9):2350. https://doi.org/10.3390/cells10092350 PMID: 34571999
17. Stroeymeyt N, Casillas-Pérez B, Cremer S. Organisational immunity in social insects. Curr Opin Insect Sci. 2014;5:1–15. https://doi.org/10.1016/j.cois.2014.09.001 PMID: 32846736
18. Cremer S, Armitage SAO, Schmid-Hempel P. Social immunity. Curr Biol. 2007;17(16):R693-702. https://doi.org/10.1016/j.cub.2007.06.008
19. Piqueret B, Sandoz J-C, d'Ettorre P. The neglected potential of invertebrates in detecting disease via olfaction. Front Ecol Evol. 2023;10. https://doi.org/10.3389/fevo.2022.960757
20. Stensmyr MC, Dweck HKM, Farhan A, Ibba I, Strutz A, Mukunda L, et al. A conserved dedicated olfactory circuit for detecting harmful microbes in *Drosophila*. Cell. 2012;151(6):1345–57. https://doi.org/10.1016/j.cell.2012.09.046 PMID: 23217715
21. Boillat M, Challet L, Rossier D, Kan C, Carleton A, Rodriguez I. The vomeronasal system mediates sick conspecific avoidance. Curr Biol. 2015;25(2):251–5. https://doi.org/10.1016/j.cub.2014.11.061 PMID: 25578906
22. Ebrahim SAM, Talross GJS, Carlson JR. Sight of parasitoid wasps accelerates sexual behavior and upregulates a micropeptide gene in *Drosophila*. Nat Commun. 2021;12(1):2453. https://doi.org/10.1038/s41467-021-22712-0 PMID: 33907186
23. Yanagawa A, Guigue AMA, Marion-Poll F. Hygienic grooming is induced by contact chemicals in *Drosophila melanogaster*. Front Behav Neurosci. 2014;8:254. https://doi.org/10.3389/fnbeh.2014.00254 PMID: 25100963
24. Yanagawa A, Neyen C, Lemaitre B, Marion-Poll F. The gram-negative sensing receptor PGRP-LC contributes to grooming induction in *Drosophila*. PLoS One. 2017;12(11):e0185370. https://doi.org/10.1371/journal.pone.0185370 PMID: 29121087
25. Zhukovskaya M, Yanagawa A, Forschler BT. Grooming behavior as a mechanism of insect disease defense. Insects. 2013;4(4):609–30. https://doi.org/10.3390/insects4040609 PMID: 26462526
26. Dziarski R. Recognition of bacterial peptidoglycan by the innate immune system. Cell Mol Life Sci. 2003;60(9):1793–804. https://doi.org/10.1007/s00018-003-3019-6 PMID: 14523544
27. Medzhitov R, Janeway C Jr. Innate immune recognition: Mechanisms and pathways. Immunol Rev. 2000;173:89–97. https://doi.org/10.1034/j.1600-065x.2000.917309.x PMID: 10719670
28. Janeway CA. How the immune system discriminates infectious nonself from noninfectious self. In: Faist E, Meakins JL, Schildberg FW, editors. Host defense dysfunction in trauma, shock and sepsis: Mechanisms and therapeutic approaches. Berlin, Heidelberg: Springer; 1993. p. 39–47. https://doi.org/10.1007/978-3-642-77405-8_5
29. Akira S, Uematsu S, Takeuchi O. Pathogen recognition and innate immunity. Cell. 2006;124(4):783–801. https://doi.org/10.1016/j.cell.2006.02.015 PMID: 16497588
30. Santoni G, Cardinali C, Morelli MB, Santoni M, Nabissi M, Amantini C. Danger- and pathogen-associated molecular patterns recognition by pattern-recognition receptors and ion channels of the transient receptor potential family triggers the inflammasome activation in immune cells and sensory neurons. J Neuroinflammation. 2015;12:21. https://doi.org/10.1186/s12974-015-0239-2 PMID: 25644504
31. Masuzzo A, Manière G, Grosjean Y, Kurz L, Royet J. Bacteria-derived peptidoglycan triggers a noncanonical nuclear factor-κB-dependent response in *Drosophila* gustatory neurons. J Neurosci. 2022;42(41):7809–23. https://doi.org/10.1523/JNEUROSCI.2437-21.2022 PMID: 36414007
32. Masuzzo A, Manière G, Viallat-Lieutaud A, Avazeri É, Zugasti O, Grosjean Y, et al. Peptidoglycan-dependent NF-κB activation in a small subset of brain octopaminergic neurons controls female oviposition. Elife. 2019;8:e50559. https://doi.org/10.7554/eLife.50559 PMID: 31661076
33. Kurata S. Peptidoglycan recognition proteins in *Drosophila* immunity. Dev Comp Immunol. 2014;42(1):36–41. https://doi.org/10.1016/j.dci.2013.06.006 PMID: 23796791
34. Kobler JM, Rodriguez Jimenez FJ, Petcu I, Grunwald Kadow IC. Immune receptor signaling and the mushroom body mediate post-ingestion pathogen avoidance. Curr Biol. 2020;30(23):4693-4709.e3. https://doi.org/10.1016/j.cub.2020.09.022 PMID: 33007248
35. Charroux B, Rival T, Narbonne-Reveau K, Royet J. Bacterial detection by *Drosophila* peptidoglycan recognition proteins. Microbes Infect. 2009;11(6–7):631–6. https://doi.org/10.1016/j.micinf.2009.03.004 PMID: 19344780
36. Fioriti F, Rifflet A, Gomperts Boneca I, Zugasti O, Royet J. Bacterial peptidoglycan serves as a critical modulator of the gut-immune-brain axis in *Drosophila*. Brain Behav Immun. 2024;119:878–97. https://doi.org/10.1016/j.bbi.2024.05.009 PMID: 38710338
37. Montanari M, Manière G, Berthelot-Grosjean M, Dusabyinema Y, Gillet B, Grosjean Y, et al. Larval microbiota primes the *Drosophila* adult gustatory response. Nat Commun. 2024;15(1):1341. https://doi.org/10.1038/s41467-024-45532-4 PMID: 38351056
38. Kurz CL, Charroux B, Chaduli D, Viallat-Lieutaud A, Royet J. Peptidoglycan sensing by octopaminergic neurons modulates *Drosophila* oviposition. Elife. 2017;6:e21937. https://doi.org/10.7554/eLife.21937 PMID: 28264763
39. Lee K-A, Kim B, Bhin J, Kim DH, You H, Kim E-K, et al. Bacterial uracil modulates *Drosophila* DUOX-dependent gut immunity via Hedgehog-induced signaling endosomes. Cell Host Microbe. 2015;17(2):191–204. https://doi.org/10.1016/j.chom.2014.12.012 PMID: 25639794

40. Joshi M, Royet J. Uridine catabolism breaks the bonds of commensalism. Cell Host Microbe. 2020;27(3):312–4. https://doi.org/10.1016/j.chom.2020.02.008 PMID: 32164840
41. Lee K-A, Kim S-H, Kim E-K, Ha E-M, You H, Kim B, et al. Bacterial-derived uracil as a modulator of mucosal immunity and gut-microbe homeostasis in *Drosophila*. Cell. 2013;153(4):797–811. https://doi.org/10.1016/j.cell.2013.04.009 PMID: 23663779
42. Kim E-K, Lee K-A, Hyeon DY, Kyung M, Jun K-Y, Seo SH, et al. Bacterial nucleoside catabolism controls quorum sensing and commensal-to-pathogen transition in the *Drosophila* gut. Cell Host Microbe. 2020;27(3):345-357.e6. https://doi.org/10.1016/j.chom.2020.01.025 PMID: 32078802
43. Benguettat O, Jneid R, Soltys J, Loudhaief R, Brun-Barale A, Osman D, et al. The DH31/CGRP enteroendocrine peptide triggers intestinal contractions favoring the elimination of opportunistic bacteria. PLoS Pathog. 2018;14(9):e1007279. https://doi.org/10.1371/journal.ppat.1007279 PMID: 30180210
44. Tleiss F, et al. Spatial and temporal coordination of Duox/TrpA1/Dh31 and IMD pathways is required for the efficient elimination of pathogenic bacteria in the intestine of *Drosophila* larvae. eLife. 2024;13. https://doi.org/10.7554/eLife.98716.2
45. Gu P, et al. Polymodal nociception in *Drosophila* requires alternative splicing of TrpA1. Curr Biol. 2019;29(23):3961-3973.e6. https://doi.org/10.1016/j.cub.2019.09.070
46. Du EJ, Ahn TJ, Wen X, Seo D-W, Na DL, Kwon JY, et al. Nucleophile sensitivity of *Drosophila* TRPA1 underlies light-induced feeding deterrence. Elife. 2016;5:e18425. https://doi.org/10.7554/eLife.18425 PMID: 27656903
47. Kwon Y, Kim SH, Ronderos DS, Lee Y, Akitake B, Woodward OM, et al. *Drosophila* TRPA1 channel is required to avoid the naturally occurring insect repellent citronellal. Curr Biol. 2010;20(18):1672–8. https://doi.org/10.1016/j.cub.2010.08.016 PMID: 20797863
48. Kim SH, Lee Y, Akitake B, Woodward OM, Guggino WB, Montell C. *Drosophila* TRPA1 channel mediates chemical avoidance in gustatory receptor neurons. Proc Natl Acad Sci U S A. 2010;107(18):8440–5. https://doi.org/10.1073/pnas.1001425107 PMID: 20404155
49. Rosenzweig M, Brennan KM, Tayler TD, Phelps PO, Patapoutian A, Garrity PA. The *Drosophila* ortholog of vertebrate TRPA1 regulates thermotaxis. Genes Dev. 2005;19(4):419–24. https://doi.org/10.1101/gad.1278205 PMID: 15681611
50. Montell C. The TRP superfamily of cation channels. Sci STKE. 2005;2005(272):re3. https://doi.org/10.1126/stke.2722005re3
51. Luo J, Shen WL, Montell C. TRPA1 mediates sensation of the rate of temperature change in *Drosophila* larvae. Nat Neurosci. 2017;20(1):34–41. https://doi.org/10.1038/nn.4416 PMID: 27749829
52. Guntur AR, Gou B, Gu P, He R, Stern U, Xiang Y, et al. H2O2-Sensitive isoforms of *Drosophila melanogaster* TRPA1 act in bitter-sensing gustatory neurons to promote avoidance of UV during egg-laying. Genetics. 2017;205(2):749–59. https://doi.org/10.1534/genetics.116.195172 PMID: 27932542
53. Soldano A, Alpizar YA, Boonen B, Franco L, López-Requena A, Liu G, et al. Gustatory-mediated avoidance of bacterial lipopolysaccharides via TRPA1 activation in *Drosophila*. Elife. 2016;5:e13133. https://doi.org/10.7554/eLife.13133 PMID: 27296646
54. Weiss LA, Dahanukar A, Kwon JY, Banerjee D, Carlson JR. The molecular and cellular basis of bitter taste in *Drosophila*. Neuron. 2011;69(2):258–72. https://doi.org/10.1016/j.neuron.2011.01.001 PMID: 21262465
55. Du EJ, Ahn TJ, Kwon I, Lee JH, Park J-H, Park SH, et al. TrpA1 regulates defecation of food-borne pathogens under the control of the duox pathway. PLoS Genet. 2016;12(1):e1005773. https://doi.org/10.1371/journal.pgen.1005773 PMID: 26726767
56. Trevisani M, Siemens J, Materazzi S, Bautista DM, Nassini R, Campi B, et al. 4-Hydroxynonenal, an endogenous aldehyde, causes pain and neurogenic inflammation through activation of the irritant receptor TRPA1. Proc Natl Acad Sci U S A. 2007;104(33):13519–24. https://doi.org/10.1073/pnas.0705923104 PMID: 17684094
57. Macpherson LJ, Dubin AE, Evans MJ, Marr F, Schultz PG, Cravatt BF, et al. Noxious compounds activate TRPA1 ion channels through covalent modification of cysteines. Nature. 2007;445(7127):541–5. https://doi.org/10.1038/nature05544 PMID: 17237762
58. Andersson DA, Gentry C, Moss S, Bevan S. Transient receptor potential A1 is a sensory receptor for multiple products of oxidative stress. J Neurosci. 2008;28(10):2485–94. https://doi.org/10.1523/JNEUROSCI.5369-07.2008 PMID: 18322093
59. Viana F. TRPA1 channels: molecular sentinels of cellular stress and tissue damage. J Physiol. 2016;594(15):4151–69. https://doi.org/10.1113/JP270935 PMID: 27079970
60. Joshi M, Viallat-Lieutaud A, Royet J. Role of Rab5 early endosomes in regulating *Drosophila* gut antibacterial response. iScience. 2023;26(8):107335. https://doi.org/10.1016/j.isci.2023.107335
61. Mi T, Mack JO, Koolmees W, Lyon Q, Yochimowitz L, Teng Z-Q, et al. Alkaline taste sensation through the alkaliphile chloride channel in *Drosophila*. Nat Metab. 2023;5(3):466–80. https://doi.org/10.1038/s42255-023-00765-3 PMID: 36941450
62. Basset A, Khush RS, Braun A, Gardan L, Boccard F, Hoffmann JA, et al. The phytopathogenic bacteria Erwinia carotovora infects *Drosophila* and activates an immune response. Proc Natl Acad Sci U S A. 2000;97(7):3376–81. https://doi.org/10.1073/pnas.97.7.3376 PMID: 10725405
63. Kim E-K, Lee K-A, Hyeon DY, Kyung M, Jun K-Y, Seo SH, et al. Bacterial nucleoside catabolism controls quorum sensing and commensal-to-pathogen transition in the *Drosophila* gut. Cell Host Microbe. 2020;27(3):345-357.e6. https://doi.org/10.1016/j.chom.2020.01.025 PMID: 32078802
64. Chakrabarti S, Poidevin M, Lemaitre B. The *Drosophila* MAPK p38c regulates oxidative stress and lipid homeostasis in the intestine. PLoS Genet. 2014;10(9):e1004659. https://doi.org/10.1371/journal.pgen.1004659 PMID: 25254641
65. Meunier N, Marion-Poll F, Rospars J-P, Tanimura T. Peripheral coding of bitter taste in *Drosophila*. J Neurobiol. 2003;56(2):139–52. https://doi.org/10.1002/neu.10235 PMID: 12838579